

1 **Convergent evolution in SARS-CoV-2 Spike creates a variant soup that causes new COVID-19
2 waves.**

3

4 Daniele Focosi^{1, #}

5 Rodrigo Quiroga²

6 Scott A. McConnell³

7 Marc C Johnson⁴

8 Arturo Casadevall³

9

10 ¹North-Western Tuscany Blood Bank, Pisa University Hospital, Pisa, Italy.

11 ²Instituto de Investigaciones en Físico-Química de Córdoba (INFIQC-CONICET), Facultad de Ciencias
12 Químicas, Universidad Nacional de Córdoba, Argentina. rquiroga@unc.edu.ar

13 ³Department of Molecular Microbiology and Immunology, Johns Hopkins Bloomberg School of Public
14 Health, Baltimore, MD, USA.

15 ⁴Department of Molecular Microbiology and Immunology, University of Missouri School of Medicine,
16 Columbia, MO, USA

17 [#]corresponding author: daniele.focosi@gmail.com .

18

19 **Word count:** abstract 177; body 3900.

20 **Author contributions:** D.F. wrote the first draft and designed Figures 3, 4, and 5; S.M. designed
21 Figure 6, R.Q. designed Figure 4. R.Q. A.C, M.C.J.. and S.M. revised the manuscript.

22 **Keywords:** SARS-CoV-2; Spike; Omicron; convergent evolution; R346; K444; BQ.1.1; XBB; Evusheld™;
23 cilgavimab; tixagevimab; bebtelovimab.

24 **Abbreviations:** IC: immunocompromised; MR: mutation rate; RBM : receptor-binding motif; VOC:
25 variant of concern.

26 **Acknowledgments:** we are grateful to Cornelius Roemer (Biozentrum - Universität Basel,
27 Switzerland), Thomas P Peacock (Imperial College, UK), independent researchers Ryan Hisner and
28 Federico Gueli, and the Twitter user @FanDorop for discussions about convergent evolution.

29 **Abstract**

30 The first 2 years of the COVID-19 pandemic were mainly characterized by convergent evolution of
31 mutations of SARS-CoV-2 Spike protein at residues K417, L452, E484, N501 and P681 across different
32 variants of concern (Alpha, Beta, Gamma, and Delta). Since Spring 2022 and the third year of the
33 pandemic, with the advent of Omicron and its sublineages, convergent evolution has led to the
34 observation of different lineages acquiring an additional group of mutations at different amino acid
35 residues, namely R346, K444, N450, N460, F486, F490, Q493, and S494. Mutations at these residues
36 have become increasingly prevalent during Summer and Autumn 2022, with combinations showing
37 increased fitness. The most likely reason for this convergence is the selective pressure exerted by
38 previous infection- or vaccine-elicited immunity. Such accelerated evolution has caused failure of all
39 anti-Spike monoclonal antibodies, including bebtelovimab and cilgavimab. While we are learning
40 how fast coronaviruses can mutate and recombine, we should reconsider opportunities for
41 economically sustainable escape-proof combination therapies, and refocus antibody-mediated
42 therapeutic efforts on polyclonal preparations that are less likely to allow for viral immune escape.

43 Introduction

44 In the third year of the COVID-19 pandemic, the majority of the general population is now largely
45 protected from severe COVID-19 disease and death by mass vaccination campaigns and by
46 immunity from former infection. Unfortunately, SARS-CoV-2 remains a life-threatening pathogen for
47 immunocompromised (IC) patients who are unable to mount a protective immune response. IC
48 individuals create a cohort population in whom the virus can persistently replicate, which is a
49 novelty for pandemics. In this regard, advancements in therapeutics and supportive care have
50 greatly increased the prevalence of IC patients compared to just a few decades ago. SARS-CoV-2
51 infection in IC patients is arguably the most difficult current problem in the COVID-19 pandemic for
52 these individuals can have large viral loads with inevitably include antigenically different viruses and
53 have a diminished capacity for clearing the infection.

54 Since Summer 2022, SARS-CoV-2 transmission has proceeded undisturbed worldwide after the
55 relaxation of nonpharmaceutical interventions such as lockdowns, social distancing, hand hygiene,
56 and face masks, which together with the waning of infection- and vaccine-elicited immunity, has
57 increased opportunities for spread and the number of susceptible individuals, respectively. Hence,
58 the increase in the “human culture medium” has led to large infectious waves during 2022, with
59 estimated excess deaths similar to those observed in 2020 [1]. While acquisition and waning of
60 immunity from former infections is not a novel occurrence, the COVID-19 pandemic has created
61 conditions whereby the natural course of a coronavirus pandemic is changed by introducing timely
62 vaccination campaigns and therapeutics targeting the viral receptor domain. There is no historical
63 precedent for the current situation. The combined action of increasing cumulative viral loads in the
64 “human culture medium” and such selective pressures has led to an unprecedented increase in viral
65 diversification in 2022. WHO nomenclature for variants of concern remained stuck at “Omicron”[2],
66 while alternative naming schemes introduced novel names to designate lineages that are
67 responsible for thousands of hospitalizations. The most refined phylogeny to date has been released
68 by PANGOLIN which counts more than 600 designated Omicron sublineages at the time of writing
69 (<https://www.pango.network/summary-of-designated-omicron-lineages/>), accounting for more than
70 45% of SARS-CoV-2 variability (Figure 1). Of interest, such increase in divergence was detected
71 despite a 75% reduction in genomic surveillance in 2022, which is mainly due to budget constraints.
72 After peaking at 1 million sequences in January 2022, the number of new sequences deposited at
73 the site decreased to 250,000 in October 2022 (<https://cov-spectrum.org/explore/World/AllSamples/Past6M/sequencing-coverage>). Consequently, it is likely
74 that the number of defined circulating sublineages is an underestimate of the viral genetic variation
75 in the current pandemic.

77 Mutation rates and mutational spectra

78 Mutation rate (MR) is often used interchangeably to indicate 2 different things: occurrence of
79 mutations within a single host (intrahost evolution at individual level without any demand for
80 outcompeting co-circulating strains) or step-wise accumulation of mutations (“antigenic drift”) that
81 get fixated within a species. While the first meaning has been demonstrated (e.g., in IC hosts[3-5],
82 and after administration of the small molecule antiviral molnupiravir which known to increase G→A
83 and C→U transition mutations[6], potentially contributing to new lineages), from an evolutionary
84 standpoint it is the second meaning which is more interesting and already well-established for other
85 respiratory pathogens[7], including the related human coronavirus 229E[8].

86 Early in the pandemic, data suggested that mass vaccination could restrict SARS-CoV-2 mutation
87 rates (MR): the diversity of the SARS-CoV-2 lineages declined at the country-level with increased rate

88 of mass vaccination ($r = -0.72$) and vaccine breakthrough patients harbor viruses with 2.3-fold lower
89 diversity in known B cell epitopes compared to unvaccinated COVID-19 patients [9]. Also, vaccination
90 coverage rate was inversely correlated to the MR of the SARS-CoV-2 Delta variant in 16 countries
91 ($r^2 = 0.878$) [10].

92 Ruis *et al* found a halving in the relative rate of G→T mutations in Omicron compared to pre-
93 Omicron sublineages[11]. To exclude selective pressures on the derived protein structures, Bloom *et*
94 *al* found similar results by repeating the analysis focusing on 4-fold degenerate codons (i.e. codons
95 that can tolerate any point mutation at the third position, although codon usage bias restricts this in
96 practice in many organisms) [12]. Replicaion of viruses and bacteria in the lower respiratory tract has
97 been associated with high levels of G>T mutations and for SARS-CoV-2 this effect occurred with
98 Delta but was lost in Omicron [11]. Such changes on mutation type and rate could theoretically stem
99 from mutations affecting genome replication and packaging [13], as well as from mutations in
100 genes encoding proteins (e.g. APOBEC) that antagonize host innate-immune factors, which
101 otherwise will mutate viral nucleic acids[14-16] and/or from environmental factors [6].

102 The average MR of the entire SARS-CoV-2 genome was estimated from the related mouse hepatitis
103 virus (MHV) to be 10^{-6} nucleotides per cycle, or 4.83×10^{-4} subs/site/year, which is similar, or slightly
104 lower, than observed for other RNA viruses [17]. Following the removal of mandatory
105 nonpharmaceutical interventions such as face masks, social distancing, and quarantine in most
106 western countries, vaccination was not sufficient to prevent hyperendemicity. The MR of SARS-CoV-
107 2 consequently doubled from 23 substitutions per year before December 2021 to 45 substitutions
108 per year after December 2021, coinciding with the advent of omicron (Figure 2), which approximates
109 14.5/subs/year for the ~30 kb SARS-CoV-2 genome. This rate should set the upper limit for mutation
110 frequency, as many mutations will not be viable and/or transmissible, and thus not observed in the
111 sequencing data at baseline. It had been previously shown that the P203L mutation in the error-
112 correcting exonuclease non-structural protein 14 (nsp14) almost doubles the genomic MR (from 20
113 to 36 SNPs/year) [18]. While this change is not prevalent in Omicron lineages, many changes in the
114 replication machinery appeared with Omicron, such as K38R, Δ1265, and A1892T in Nsp3; P132H in
115 Nsp5; I189V in Nsp6; P323L in Nsp12; and I42V in Nsp14, and some of them could have contributed
116 to the MR jump[19].

117 Convergent evolution

118 In the midst of such massive lineage divergence, convergent evolution towards certain motifs has
119 become increasingly manifest.

120 In the pre-Omicron and pre-vaccine era, variants of concern (VOCs) notably converged to mutations
121 which resulted in the following amino acid changes: K417N, L452R, E484K, N501Y, and P681X[20].
122 These amino acid changes have been proposed to increase the stability of the trimeric protein[21-
123 23], and they emerged in the absence of significant selective pressures by the immune system.
124 K417N, E484A, N501Y and P681H remained hallmarks of BA.2.*, while the paraphyletic BA.4/5
125 acquired L452R and F486V and the Q493R reversion.

126 In the last year the BA.2 variant first generated a wave that led first to the paraphyletic BA.4/5
127 sublineage, which was later joined by a return of so-called “second-generation” BA.2 sublineages
128 (Figure 3), with BA.2.75.* and BA.2.3.20 being the most circulated. Since Summer 2022, each of
129 those sublineages has amazingly converged with changes at the receptor-binding domain (RBD)
130 residues R346, K444, L452, N450, N460, F486, F490, Q493, and S494 (see Supplementary Table
131 1)[24]. E484A remained instead stable, with 484K never detected, A484G seen only in BA.2.3.20, and

132 A484T seen only in XBB.1.3. More recently, convergence in indels within the N-terminal domain
133 (NTD), as previously recognized in Brazilian VOCs[25], was reported for Omicron sublineages: in
134 particular, Y144del has been found in BA.4.6.3, BJ.1, BU.1, BQ.1.8.*, BQ.1.1.10, BQ.1.1.20, BQ.1.18,
135 and XBB.*)[26].

136 This “variant soup” can be organized and stratified according to the number of key Spike mutations
137 present, and although the number of key mutations acquired correlates well with increasing fitness,
138 this is only so within each lineage, which shows that the biology of SARS-CoV-2 infection goes
139 beyond what occurs in the Spike protein (Figure 4). At present, only the BQ.1-derived lineages with 7
140 or more selected mutations display a clear relative growth advantage relative comparison to the
141 BQ.1.1 baseline. Convergence was clearly observed at the amino acid level, with different nucleotide
142 mutations leading to similar amino acid changes: e.g., N460K was caused by T22942A in BQ.1*, XAW
143 and some of the BA.5.2 sublineages, while it was caused by T22942G in BA.2.75*(all lineages),
144 BA.2.3.20, BS.1, BU.1, XBB, XAK and BW.1 (BA.5.6.2.1). Another impressive example of this
145 convergent evolution is the Spike of BA.4.6.3, BQ.1.18 and BQ.1.1.20 independently acquiring the
146 following amino acid changes since their last shared common ancestor: Y144del, R346T, N460K,
147 L452R, F486V and the R493Q reversion. Also, BA.4.6.3 has acquired K444N, while BQ.1.18 and
148 BQ.1.1.20 acquired K444T.

149 **Escalating immune escape**

150 SARS-CoV-2 evolution represents an accelerated movie of Darwinian selection. Variants that are
151 more likely to escape vaccine- and infection-elicited immunity that are more fit expand at the
152 expense of those less fit. While it may sound obvious, we now have formal evidence of such
153 evolution, with PANGOLIN descendants invariably having increased RBD immune escape scores
154 compared to parental strains (Figure 5). In this ongoing race, descendants invariably replace parents,
155 as these are fitter in hosts with pre-existing immunity. In this regard, the chances for saltations
156 lineages that emerged after intrahost evolution in IC patients (i.e. in the absence of RBD immune
157 escape) seem minimal: accordingly, despite the initial hypothesis of intrahost evolution to explain
158 the saltation seen with the emergence of Omicron, recent evidence suggests that Omicron
159 ancestors circulated undetected long before the exponential spread [27].

160 RBD immune escape can nowadays be estimated *in silico* based on *in vitro* data
161 (https://jbloomlab.github.io/SARS2_RBD_Ab_escape_maps/escape-calc/). RBD immune escape is
162 clearly a moving scale with an evolving asymptote. E.g., by changing vaccine composition [28] we are
163 likely to reset the “game”.

164

165 **ACE2 affinity fine tuning**

166 ACE2 affinity can be estimated *in silico* (https://github.com/jbloomlab/SARS-CoV-2-RBD_DMS_Omicron/blob/main/results/final_variant_scores/final_variant_scores.csv). Several
167 Omicron sublineages showed remarkable examples of further evolution at Spike residues that were
168 already recently mutated. E.g.,

- 170 • BQ.1 already had K444T inherited from BE.1.1.1, but further mutated into 444M in the child
171 BQ.1.1.17
- 172 • XBB.1 already had E484A inherited from the BA.2 parent, but further mutated into 484T in
173 the child XBB.1.3

- 174 • BA.2.3 already had E484A inherited from the BA.2 parent, but further mutated into 484G in
175 the child BA.2.3.20, which caused an impressive increase in ACE2 affinity (to whom K444R,
176 L452M, and N460K contributed)
- 177 • BM.4.1.1 already had F486S inherited from the BM.4.1 parent but further mutated into
178 486P in CH.3
- 179 • BM.1.1.1 already had F486S inherited from the BM.1 parent but further mutated into 486P
180 in the child CJ.1
- 181 • XBB.1 already had F486S inherited from the BM.1.1.1 parent but further mutated into 486P
182 in the child XBB.1.5
- 183 • BA.2.75.2 already had F486S inherited from the BA.2.75 parent, but further mutated into
184 486L in the child CA.4
- 185 • BA.5.2.1 already had F486V inherited since BA.5, but further mutated to 486I in BF.12
- 186 • BW.1 already had F486V inherited from the BA.5 parent, but further mutated into 486S in
187 the child BW.1.1

188 Seven of these examples manifest escalating affinities for ACE2, with the other 2 representing no
189 change in ACE2 affinity (Figure 6).

190

191 **Mutually exclusive mutations**

192 Mutually exclusive mutations across the entire SARS-CoV-2 genome have been previously
193 studied[29], but the vast constellation of Omicron sublineages provides an unique opportunity for an
194 in-depth exploration of substitutions that are incompatible in combination. The best examples so far
195 are N450X and R346X mutations, which have not yet been observed together in more than 6 millions
196 of Omicron sequences. Two dipolar interactions exist between the carboxamide group of Asn and
197 the guanidino group of Arg in the ancestral sequence, stabilizing the receptor binding module (RBM)
198 tertiary fold (Figure 7, left). R346 resides within a short loop between helix α 1 and beta strand 1.
199 N450 is a constituent of the extended RBM insertion into the overall five-stranded antiparallel beta-
200 sheet fold of the domain. As the RBM is the critical determinant for the interaction with ACE2,
201 maintaining its optimal conformation through this stabilizing bond is likely to be essential for
202 pathogenesis. N450D is a common substitution among Omicron lineages. This mutation would result
203 in a similarly sized sidechain but different electrostatic properties (carboxamide \rightarrow carboxylic acid).
204 This substitution would likely result in a stronger interaction with position 450, as one H-bonding is
205 maintained, and one is replaced with ionic salt bridge between the deprotonated oxygen and the
206 basic guanidino group, provided that the residue at position 346 remains Arg. On the other hand,
207 any substitution at position 346, with the exception of Lys, would result in a significantly shorter,
208 non-cationic sidechain, which would abrogate this RBM-stabilizing interaction. R346K would partially
209 maintain this interaction, replacing a bidentate linkage to N450 with a monodentate dipolar
210 interaction. Thus, the observed mutual exclusivity of mutations at these two sites can be rationalized
211 by their contributions to this stabilizing intradomain interaction.

212 Other combinations have been exceedingly rare so far, and seen only in cryptic lineages (e.g., F486P
213 and K444 mutations), but no steric justifications can be found for them.

214 **Epistasis**

215 While the focus so far has been mostly on the Spike protein, it is likely that convergent evolution is
216 acting on genes other than Spike. Given that the Spike protein is the best protective antigen for both

217 infection and vaccines, mutations in other genes are more likely to provide fitness advantages if they
218 affect Spike expression. E.g., ORF8 limits the amount of Spike proteins that reaches the cell surface
219 and is incorporated into virions, reducing recognition by anti-SARS-CoV-2 antibodies[30]. ORF8 has
220 accordingly been target of convergent evolution in Omicron (e.g., ORF8:S667F in BR.2.1, ORF8:G8x in
221 XBB.1) and in SARS-related coronaviruses[31].

222 Other genes whose roles in Spike modulation are not clear are also converging, such as
223 ORF1b:T1050, found in many BA.5.2.* sublineages, and XBE (T1050N) as well as XBC.* (T1050I).

224

225 **Selective pressures from therapeutics targeting the Spike 226 protein.**

227 There is a theoretical concern that, in addition to vaccines- and infection-elicited immunity, selective
228 pressure by prophylactic and therapeutic anti-Spike monoclonal antibodies (mAb), can contribute to
229 the emergence of novel SARS-CoV-2 sublineages [32]. While selective pressures are likely to generate
230 many different mutants, a very few of those emerging sublineages could be fit enough to compete
231 with the lineages that are dominating at that time to become locally or globally dominant.

232 While spontaneous evolution can occur in the absence of selective pressures due to the intrinsic
233 genomic MR (see section above), extended half-life mAbs (such as Evusheld™) administered for pre-
234 exposure prophylaxis or therapy to chronically infected immunocompromised patients at
235 subneutralizing concentrations provide ideal conditions to facilitate the emergence of mutants[33],
236 for these patients often cannot clear the infection and have high viral loads. Establishing a cause-
237 effect relationship is difficult, but intra-host evolution studies provide a highly suggestive temporal
238 association[34]. mAbs have come of age since the advent of the SARS-CoV-2 Delta VOC, but because
239 of the resistance of Omicron to most authorized mAbs, their use since Spring 2022 has been largely
240 limited to Evusheld™ (for which cilgavimab was the only ingredient with residual activity) and
241 bebtelovimab.

242 We know from *in vitro* deep mutational scanning studies the exact mutations that cause resistance
243 to each mAb. S:F486X mutations impart resistance to tixagevimab, S:R346X, S:K444X and S:S494X
244 mutations impart resistance to cilgavimab, while S:K444X mutations impart resistance to
245 bebtelovimab (Table 1). We recently noted an increase in the circulation of Omicron sublineages
246 associated with S:R346X mutations, and wondered whether this could partly be the result of
247 selective pressure with Evusheld™. We compared the prevalence of R346X mutations in countries
248 with high versus low usage of Evusheld™ (France vs. UK) or bebtelovimab (USA vs. UK) (Figure 8). UK
249 also represents an ideal control because of its very high SARS-CoV-2 genome sequencing rate. We
250 discuss these 2 scenarios in details below.

251

252 **S:R346X**

253 Different mutations can affect the R346 residue. R346G has been selected *in vitro* by
254 cilgavimab+tixagevimab[35]. R346S occurred *in vitro* after 12 weeks of propagating SARS-CoV-2 in
255 the presence of sotrovimab, and before the other epitope mutation (P337L) which leads to
256 sotrovimab resistance [36]. R346I has been selected *in vitro* under the selective pressure from
257 cilgavimab [37,38]. Lee *et al* reported mutually exclusive substitutions at residues R346 (R346S and
258 R346I) and E484 (E484K and E484A) of Spike protein and continuous turnover of these substitutions
259 in 2 immunosuppressed patients[39]. Unfortunately, *in vivo* selection evidences are so far available

260 for sotrovimab[40] but not for Evusheld™. It should be anyway noted that R346T[41,42] and R346I[43]
261 have been reported to spontaneously develop and fix in 3 IC patients without any selective pressure.

262 While R346K was associated with the BA.1.1 wave (see Figure 8), the plethora of different Omicron
263 sublineages that showed convergent evolution towards R346I, R346S or R346T is of concern.

264 • R346K (previously seen only in VOC Mu/B.1.621 [44]) occurred exclusively in BA.1.1, a
265 sublineage that disappeared since May 2022, where it affected the interaction network in
266 the BA.1.1 RBD/hACE2 interface through long-range alterations and contributes to the
267 higher hACE2 affinity of the BA.1.1 RBD than the BA.1 RBD [45], and had increased resistance
268 against Evusheld™[46] and sotrovimab[47]. Only STI-9167 remained effective among the
269 mAbs[48]. Beta+R346K, which was identified in the Philippines in August 2021, exhibited the
270 highest resistance to 2 BNT61b2 doses-elicited sera among the tested VOCs[49]. After
271 BA.1.1, R346K has not been detected worldwide in any sublineage.

272 • R346I occurs in more than 40 different Omicron sublineages, but it is most represented in
273 BA.5.9 (38%), BA.4.1 (5%), BA.5.9 (4%), but also occurred in AY.39 (14%);

274 • R346S (previously seen only in a C.36.3 sublineage from Italy[50] (30.8%), occurs in more
275 than 40 different Omicron sublineages but it is most represented in B.1.640.1 (18%), and in a
276 few Delta sublineages (<2%) occurs nowadays in BA.4.7 (13%), BA.5.2.1 (8.22%), BA.4
277 (2.8%).

278 • R346T occurs in more than 96 different Omicron sublineages, but it is mostly represented in
279 BA.4.6 (44%), BA.5.2.1 (13%), BA.2 (8%), BA.2.74 (3%), BA.2.76 (12%), BA.4.1 (2.3%). In
280 addition, it is a hallmark mutation of BA.1.23, BA.2.9.4, BL.1, BA.2.75.2, BA.2.80, BA.2.82,
281 BA.4.1.8, BF.7 and BF.11. BA.4.6, BA.4.7, and BA.5.9 displayed higher humoral immunity
282 evasion capability than BA.4/BA.5, causing 1.5 to 1.9-fold decrease in NT_{50} of the plasma
283 from BA.1 and BA.2 breakthrough-infection convalescents compared to BA.4/BA.5.
284 Importantly, plasma from BA.5 breakthrough-infection convalescents also exhibits significant
285 neutralization activity decrease against BA.4.6, BA.4.7, and BA.5.9 than BA.4/BA.5, showing
286 on average 2.4 to 2.6-fold decrease in NT_{50} . R346S causes resistance to class 3 antibodies:
287 bebtelovimab remains potent, while Evusheld™ is completely escaped by these subvariants
288 [51].

289

290 S:K444X

291 The K444E/R mutations were reported *in vitro* after selection with cilgavimab[38]. Resistance studies
292 with bebtelovimab selected the K444T escape mutations for BA.2[52]. Ortega *et al* found that K444R
293 (previously found in the Beta VOC[53]), K444Q, and K444N mutations can change the virus binding
294 affinity to the ACE2 receptor[54]. Weisblum *et al* found that K444R/Q/N occurs after exposure to
295 convalescent plasma[55]. Among largely diversified VOCs such as Delta, S:K444N was associated with
296 reduced remdesivir binding and increased mortality[56].

297

298 Conclusions

299 The convergent evolution of Omicron sublineages appears to reflect the selective pressure exerted
300 by previous infection- or vaccine-elicited immunity. Vaccines and perhaps antibody therapeutics
301 have without doubt saved an untold number of lives but also likely altered the natural evolutionary
302 trajectory of the virus. While other viruses such as influenza and HIV routinely produced new
303 variants because of their mutagenicity, the scale at which SARS-CoV-2 has spun off new variants and

304 lineages appears unprecedented in modern virology history. The SARS-CoV-2 vaccines reduce severe
305 disease and mortality but do not confer sufficient immunity to prevent re-infection with viral
306 replication in vaccinated hosts. Hence, we have the unusual situation of viral replication in immune
307 hosts where the immune system is placing evolutionary pressure on the virus to select variants that
308 can escape vaccine-elicited immunity in addition to infection-elicited immunity. Whether this rapid
309 evolutionary trajectory is the result of viral replication properties, replication in immune hosts or
310 both is unknown but conditions present in the past year of the pandemic have produced a
311 remarkable natural experiment in viral evolution for which we cannot discern its conclusion.

312 Insights from structural biology has shown how some mutations are mutually exclusive, which could
313 help the design of next-generation vaccines. But the latter could reset the run for immune escape,
314 perpetuating the never-ending game of host and pathogen. Viral recombination[57] (more than 50
315 lineages censed at the time of writing, with both simple and complex variants[58]) and sudden
316 reemergence of former VOCs[59] have to be considered as further drivers for evolutionary saltation.

317 In this setting, polyclonal passive immunotherapies (such as plasma from convalescent and
318 vaccinated donors[60,61]) appear more escape-resistant than monoclonal antibodies[62-65], and
319 combo therapies should be urgently investigated and deployed in vulnerable populations, such as IC
320 patients[66].

321

322 **References**

- 323 1. Daily new confirmed COVID-19 deaths per million people. Our world in data. Accessed online
324 at https://ourworldindata.org/explorers/coronavirus-data-explorer?zoomToSelection=true&time=2020-03-01..latest&facet=none&pickerSort=asc&pickerMetric=location&hideControls=false&Metric=Confirmed+deaths&Interval=7-day+rolling+average&Relative+to+Population=true&Color+by+test+positivity=false&country=~OWID_WRL on December 1, 2022.
- 325 2. Viana, R.; Moyo, S.; Amoako, D.G.; Tegally, H.; Scheepers, C.; Althaus, C.L.; Anyaneji, U.J.;
326 Bester, P.A.; Boni, M.F.; Chand, M.; et al. Rapid epidemic expansion of the SARS-CoV-2
327 Omicron variant in southern Africa. *Nature* **2022**, *603*, 679-686, doi:10.1038/s41586-022-04411-y.
- 328 3. Harari, S.; Tahor, M.; Rutsinsky, N.; Meijer, S.; Miller, D.; Henig, O.; Halutz, O.; Levytskyi, K.;
329 Ben-Ami, R.; Adler, A.; et al. Drivers of adaptive evolution during chronic SARS-CoV-2
330 infections. *Nat Med* **2022**, *28*, 1501-1508, doi:10.1038/s41591-022-01882-4.
- 331 4. Kemp, S.A.; Collier, D.A.; Datir, R.P.; Ferreira, I.A.T.M.; Gayed, S.; Jahun, A.; Hosmillo, M.;
332 Rees-Spear, C.; Mlcochova, P.; Lumb, I.U.; et al. SARS-CoV-2 evolution during treatment of
333 chronic infection. *Nature* **2021**, *592*, 277-282, doi:10.1038/s41586-021-03291-y.
- 334 5. Wilkinson, S.A.J.; Richter, A.; Casey, A.; Osman, H.; Mirza, J.D.; Stockton, J.; Quick, J.;
335 Ratcliffe, L.; Sparks, N.; Cumley, N.; et al. Recurrent SARS-CoV-2 mutations in
336 immunodeficient patients. *Virus Evol* **2022**, *8*, veac050, doi:10.1093/ve/veac050.
- 337 6. Focosi, D. Molnupiravir: From Hope to Epic Fail? **2022**, *14*, 2560.
- 338 7. Smith, D.J.; Lapedes, A.S.; de Jong, J.C.; Bestebroer, T.M.; Rimmelzwaan, G.F.; Osterhaus,
339 A.D.; Fouchier, R.A. Mapping the antigenic and genetic evolution of influenza virus. *Science*
340 **2004**, *305*, 371-376, doi:10.1126/science.1097211.
- 341 8. Eguia, R.T.; Crawford, K.H.D.; Stevens-Ayers, T.; Kelnhofer-Millevolte, L.; Greninger, A.L.;
342 Englund, J.A.; Boeckh, M.J.; Bloom, J.D. A human coronavirus evolves antigenically to escape
343 antibody immunity. *PLoS Pathog* **2021**, *17*, e1009453, doi:10.1371/journal.ppat.1009453.

350 9. Niesen, M.; Anand, P.; Silvert, E.; Suratekar, R.; Pawlowski, C.; Ghosh, P.; Lenehan, P.;
351 Hughes, T.; Zemmour, D.; OHoro, J.C.; et al. COVID-19 vaccines dampen genomic diversity of
352 SARS-CoV-2: Unvaccinated patients exhibit more antigenic mutational variance. **2021**,
353 2021.2007.2001.21259833, doi:10.1101/2021.07.01.21259833 %J medRxiv.
354 10. Yeh, T.-Y.; Contreras, G.P. Full vaccination is imperative to suppress SARS-CoV-2 delta variant
355 mutation frequency. **2021**, 2021.2008.2008.21261768, doi:10.1101/2021.08.08.21261768
356 %J medRxiv.
357 11. Ruis, C.; Peacock, T.P.; Polo, L.M.; Masone, D.; Alvarez, M.S.; Hinrichs, A.S.; Turakhia, Y.;
358 Cheng, Y.; McBroome, J.; Corbett-Detig, R.; et al. Mutational spectra distinguish SARS-CoV-2
359 replication niches. **2022**, 2022.2009.2027.509649, doi:10.1101/2022.09.27.509649 %J
360 bioRxiv.
361 12. Bloom, J.D.; Beichman, A.C.; Neher, R.A.; Harris, K. Evolution of the SARS-CoV-2 mutational
362 spectrum. **2022**, 2022.2011.2019.517207, doi:10.1101/2022.11.19.517207 %J bioRxiv.
363 13. V'Kovski, P.; Kratzel, A.; Steiner, S.; Stalder, H.; Thiel, V. Coronavirus biology and replication:
364 implications for SARS-CoV-2. *Nature reviews. Microbiology* **2021**, 19, 155-170,
365 doi:10.1038/s41579-020-00468-6.
366 14. Sadler, H.A.; Stenglein, M.D.; Harris, R.S.; Mansky, L.M. APOBEC3G contributes to HIV-1
367 variation through sublethal mutagenesis. *Journal of virology* **2010**, 84, 7396-7404,
368 doi:10.1128/jvi.00056-10.
369 15. De Maio, N.; Walker, C.R.; Turakhia, Y.; Lanfear, R.; Corbett-Detig, R.; Goldman, N. Mutation
370 Rates and Selection on Synonymous Mutations in SARS-CoV-2. *Genome biology and*
371 *evolution* **2021**, 13, doi:10.1093/gbe/evab087.
372 16. Ratcliff, J.; Simmonds, P. Potential APOBEC-mediated RNA editing of the genomes of SARS-
373 CoV-2 and other coronaviruses and its impact on their longer term evolution. *Virology* **2021**,
374 556, 62-72, doi:10.1016/j.virol.2020.12.018.
375 17. Mercatelli, D.; Giorgi, F.M. Geographic and Genomic Distribution of SARS-CoV-2 Mutations.
376 **2020**, 11, doi:10.3389/fmicb.2020.01800.
377 18. Takada, K.; Ueda, M.T.; Watanabe, T.; Nakagawa, S. Genomic diversity of SARS-CoV-2 can be
378 accelerated by a mutation in the nsp14 gene. **2020**, 2020.2012.2023.424231,
379 doi:10.1101/2020.12.23.424231 %J bioRxiv.
380 19. Jung, C.; Kmiec, D.; Koepke, L.; Zech, F.; Jacob, T.; Sparrer, K.M.J.; Kirchhoff, F. Omicron:
381 What Makes the Latest SARS-CoV-2 Variant of Concern So Concerning? **2022**, 96, e02077-
382 02021, doi:doi:10.1128/jvi.02077-21.
383 20. Focosi, D. SARS-CoV-2 Spike protein convergent evolution 2021.
384 21. Neto, D.F.L.; Fonseca, V.; Jesus, R.; Dutra, L.H.; Portela, L.M.O.; Freitas, C.; Fillizola, E.;
385 Soares, B.; Abreu, A.L.; Twiari, S.; et al. Molecular dynamics simulations of the SARS-CoV-2
386 Spike protein and variants of concern: structural evidence for convergent adaptive
387 evolution. *Journal of biomolecular structure & dynamics* **2022**, 1-13,
388 doi:10.1080/07391102.2022.2097955.
389 22. Upadhyay, V.; Patrick, C.; Lucas, A.; Mallela, K.M.G. Convergent Evolution of Multiple
390 Mutations Improves the Viral Fitness of SARS-CoV-2 Variants by Balancing Positive and
391 Negative Selection. *Biochemistry* **2022**, 61, 963-980, doi:10.1021/acs.biochem.2c00132.
392 23. Martin, D.P.; Weaver, S.; Tegally, H.; San, J.E.; Shank, S.D.; Wilkinson, E.; Lucaci, A.G.;
393 Giandhari, J.; Naidoo, S.; Pillay, Y.; et al. The emergence and ongoing convergent evolution of
394 the SARS-CoV-2 N501Y lineages. *Cell* **2021**, 184, 5189-5200.e5187,
395 doi:10.1016/j.cell.2021.09.003.
396 24. Variant report 2022-09-14. Accessed online at https://github.com/neherlab/SARS-CoV-2_variant-reports/blob/main/reports/variant_report_2022-09-14.md on November 23,
397 2022.
398 25. Resende, P.C.; Naveca, F.G.; Lins, R.D.; Dezordi, F.Z.; Ferraz, M.V.F.; Moreira, E.G.; Coêlho,
399 D.F.; Motta, F.C.; Paixão, A.C.D.; Appolinario, L.; et al. The ongoing evolution of variants of

401 concern and interest of SARS-CoV-2 in Brazil revealed by convergent indels in the amino (N)-
402 terminal domain of the spike protein. *Virus Evol* **2021**, *7*, veab069, doi:10.1093/ve/veab069.
403 26. Cao, Y.; Jian, F.; Wang, J.; Yu, Y.; Song, W.; Yisimayi, A.; Wang, J.; An, R.; Zhang, N.; Wang, Y.;
404 et al. Imprinted SARS-CoV-2 humoral immunity induces convergent Omicron RBD evolution.
405 **2022**, 2022.2009.2015.507787, doi:10.1101/2022.09.15.507787 %J bioRxiv.
406 27. Fischer, C.; Maponga, T.G.; Yadouleton, A.; Abílio, N.; Aboce, E.; Adewumi, P.; Afonso, P.;
407 Akorli, J.; Andriamandimby, S.F.; Anga, L.; et al. Gradual emergence followed by exponential
408 spread of the SARS-CoV-2 Omicron variant in Africa. *O*, eadd8737,
409 doi:doi:10.1126/science.add8737.
410 28. Focosi, D.; Maggi, F. Do We Really Need Omicron Spike-Based Updated COVID-19 Vaccines?
411 Evidence and Pipeline. *Viruses* **2022**, *14*, doi:10.3390/v14112488.
412 29. Al Khalaf, R.; Bernasconi, A.; Pinoli, P.; Ceri, S. Analysis of co-occurring and mutually exclusive
413 amino acid changes and detection of convergent and divergent evolution events in SARS-
414 CoV-2. *Computational and structural biotechnology journal* **2022**, *20*, 4238-4250,
415 doi:10.1016/j.csbj.2022.07.051.
416 30. Kim, I.-J.; Lee, Y.-h.; Khalid, M.M.; Zhang, Y.; Ott, M.; Verdin, E. SARS-CoV-2 ORF8 limits
417 expression levels of Spike antigen. **2022**, 2022.2011.2009.515752,
418 doi:10.1101/2022.11.09.515752 %J bioRxiv.
419 31. Akaishi, T.; Fujiwara, K.; Ishii, T. Insertion/deletion hotspots in the Nsp2, Nsp3, S1, and ORF8
420 genes of SARS-related coronaviruses. *BMC ecology and evolution* **2022**, *22*, 123,
421 doi:10.1186/s12862-022-02078-7.
422 32. Focosi, D.; McConnell, S.; Casadevall, A.; Cappello, E.; Valdiserra, G.; Tuccori, M. Monoclonal
423 antibody therapies against SARS-CoV-2. *The Lancet Infectious Diseases* **2022**, *22*, 00311-
424 00315, doi:10.1016/S1473-3099(22)00311-5.
425 33. Focosi, D.; Casadevall, A. A Critical Analysis of the Use of Cilgavimab plus Tixagevimab
426 Monoclonal Antibody Cocktail (Evusheld®) for COVID19 Prophylaxis and Treatment.
427 **2022**, *14*, 1999.
428 34. Focosi, D.; Maggi, F.; Franchini, M.; McConnell, S.; Casadevall, A. Analysis of Immune Escape
429 Variants from Antibody-Based Therapeutics against COVID-19: A Systematic Review.
430 *International journal of molecular sciences* **2022**, *23*, 29.
431 35. Copin, R.; Baum, A.; Wloga, E.; Pascal, K.E.; Giordano, S.; Fulton, B.O.; Zhou, A.; Negron, N.;
432 Lanza, K.; Chan, N.; et al. The monoclonal antibody combination REGEN-COV protects
433 against SARS-CoV-2 mutational escape in preclinical and human studies. *Cell* **2021**, *184*,
434 3949-3961, doi: 10.1016/j.cell.2021.06.002.
435 36. Magnus, C.L.; Hiergeist, A.; Schuster, P.; Rohrhofer, A.; Medenbach, J.; Gessner, A.;
436 Peterhoff, D.; Schmidt, B. Targeted escape of SARS-CoV-2 in vitro from monoclonal antibody
437 S309, the precursor of sotrovimab. *Frontiers in immunology* **2022**, *13*, 966236,
438 doi:10.3389/fimmu.2022.966236.
439 37. Dong, J.; Zost, S.J.; Greaney, A.J.; Starr, T.N.; Dingens, A.S.; Chen, E.C.; Chen, R.E.; Case, J.B.;
440 Sutton, R.E.; Gilchuk, P.; et al. Genetic and structural basis for SARS-CoV-2 variant
441 neutralization by a two-antibody cocktail. *Nat Microbiol* **2021**, *6*, 1233-1244,
442 doi:10.1038/s41564-021-00972-2.
443 38. FDA. Fact sheet for healthcare providers: emergency use authorization for Evusheld™
444 (tixagevimab co-packaged with cilgavimab). Accessed online at
445 <https://www.fda.gov/media/154701/download> on August 13, 2022. **2021**.
446 39. Lee, J.S.; Yun, K.W.; Jeong, H.; Kim, B.; Kim, M.J.; Park, J.H.; Shin, H.S.; Oh, H.S.; Sung, H.;
447 Song, M.G.; et al. SARS-CoV-2 shedding dynamics and transmission in immunosuppressed
448 patients. *Virulence* **2022**, *13*, 1242-1251, doi:10.1080/21505594.2022.2101198.
449 40. Andrés, C.; González-Sánchez, A.; Jiménez, M.; Márquez-Algabea, E.; Piñana, M.; Fernández-
450 Naval, C.; Esperalba, J.; Saubi, N.; Quer, J.; Rando-Segura, A.; et al. Emergence of Delta and
451 Omicron variants carrying resistance-associated mutations in immunocompromised patients

452 undergoing Sotrovimab treatment with long viral excretion. *Clinical microbiology and*
453 *infection : the official publication of the European Society of Clinical Microbiology and*
454 *Infectious Diseases* **2022**, doi:10.1016/j.cmi.2022.08.021.

455 41. Gonzalez-Reiche, A.S.; Alshammary, H.; Schaefer, S.; Patel, G.; Polanco, J.; Amoako, A.A.;
456 Rooker, A.; Cognigni, C.; Floda, D.; van de Guchte, A.; et al. Intra-host evolution and forward
457 transmission of a novel SARS-CoV-2 Omicron BA.1 subvariant. **2022**,
458 2022.2005.2025.22275533, doi:10.1101/2022.05.25.22275533 %J medRxiv.

459 42. Lee, C.Y.; Shah, M.K.; Hoyos, D.; Solovyov, A.; Douglas, M.; Taur, Y.; Maslak, P.; Babady, N.E.;
460 Greenbaum, B.; Kamboj, M.; et al. Prolonged SARS-CoV-2 Infection in Patients with
461 Lymphoid Malignancies. *Cancer discovery* **2022**, *12*, 62-73, doi:10.1158/2159-8290.Cd-21-
462 1033.

463 43. Sonnleitner, S.T.; Prelog, M.; Sonnleitner, S.; Hinterbichler, E.; Halbfurter, H.; Kopecky,
464 D.B.C.; Almanzar, G.; Koblmüller, S.; Sturmbauer, C.; Feist, L.; et al. Cumulative SARS-CoV-2
465 mutations and corresponding changes in immunity in an immunocompromised patient
466 indicate viral evolution within the host. *Nat Commun* **2022**, *13*, 2560, doi:10.1038/s41467-
467 022-30163-4.

468 44. Fratev, F. R346K Mutation in the Mu Variant of SARS-CoV-2 Alters the Interactions with
469 Monoclonal Antibodies from Class 2: A Free Energy Perturbation Study. *Journal of chemical*
470 *information and modeling* **2022**, *62*, 627-631, doi:10.1021/acs.jcim.1c01243.

471 45. Li, L.; Liao, H.; Meng, Y.; Li, W.; Han, P.; Liu, K.; Wang, Q.; Li, D.; Zhang, Y.; Wang, L.; et al.
472 Structural basis of human ACE2 higher binding affinity to currently circulating Omicron SARS-
473 CoV-2 sub-variants BA.2 and BA.1.1. *Cell* **2022**, *185*, 2952-2960.e2910,
474 doi:10.1016/j.cell.2022.06.023.

475 46. Uraki, R.; Kiso, M.; Imai, M.; Yamayoshi, S.; Ito, M.; Fujisaki, S.; Takashita, E.; Ujie, M.;
476 Furusawa, Y.; Yasuhara, A.; et al. Therapeutic efficacy of monoclonal antibodies and
477 antivirals against SARS-CoV-2 Omicron BA.1 in Syrian hamsters. *Nat Microbiol* **2022**, *7*, 1252-
478 1258, doi:10.1038/s41564-022-01170-4.

479 47. Nutalai, R.; Zhou, D.; Tuekprakhon, A.; Ginn, H.M.; Supasa, P.; Liu, C.; Huo, J.; Mentzer, A.J.;
480 Duyvesteyn, H.M.E.; Dijokaite-Guraliuc, A.; et al. Potent cross-reactive antibodies following
481 Omicron breakthrough in vaccinees. *Cell* **2022**, *185*, 2116-2131.e2118,
482 doi:10.1016/j.cell.2022.05.014.

483 48. Duty, J.A.; Kraus, T.; Zhou, H.; Zhang, Y.; Shaabani, N.; Yildiz, S.; Du, N.; Singh, A.; Miorin, L.;
484 Li, D.; et al. Discovery of a SARS-CoV-2 Broadly-Acting Neutralizing Antibody with Activity
485 against Omicron and Omicron + R346K Variants. **2022**, 2022.2001.2019.476998,
486 doi:10.1101/2022.01.19.476998 %J bioRxiv.

487 49. Koyama, T.; Miyakawa, K.; Tokumasu, R.; S, S.J.; Kudo, M.; Ryo, A. Evasion of vaccine-induced
488 humoral immunity by emerging sub-variants of SARS-CoV-2. *Future microbiology* **2022**, *17*,
489 417-424, doi:10.2217/fmb-2022-0025.

490 50. Castelli, M.; Baj, A.; Criscuolo, E.; Ferrarese, R.; Diotti, R.; Sampaolo, M.; Novazzi, F.; Dalla
491 Gasperina, D.; Focosi, D.; Locatelli, M.; et al. Characterization of a lineage C.36 SARS-CoV-2
492 isolate with reduced susceptibility to neutralization circulating in Lombardy, Italy. *Viruses*
493 **2021**.

494 51. Jian, F.; Yu, Y.; Song, W.; Yisimayi, A.; Yu, L.; Gao, Y.; Zhang, N.; Wang, Y.; Shao, F.; Hao, X.; et
495 al. Further humoral immunity evasion of emerging SARS-CoV-2 BA.4 and BA.5 subvariants.
496 **2022**, 2022.2008.2009.503384, doi:10.1101/2022.08.09.503384 %J bioRxiv.

497 52. Turelli, P.; Fenwick, C.; Raclot, C.; Genet, V.; Pantaleo, G.; Trono, D. P2G3 human monoclonal
498 antibody neutralizes SARS-CoV-2 Omicron subvariants including BA.4 and BA.5 and
499 Bebtelovimab escape mutants. **2022**, 2022.2007.2028.501852,
500 doi:10.1101/2022.07.28.501852 %J bioRxiv.

501 53. Umair, M.; Ikram, A.; Salman, M.; Haider, S.A.; Badar, N.; Rehman, Z.; Ammar, M.; Rana,
502 M.S.; Ali, Q. Genomic surveillance reveals the detection of SARS-CoV-2 delta, beta, and

503 gamma VOCs during the third wave in Pakistan. *Journal of medical virology* **2022**, *94*, 1115-1129, doi:10.1002/jmv.27429.

504 54. Ortega, J.T.; Pujol, F.H.; Jastrzebska, B.; Rangel, H.R. Mutations in the SARS-CoV-2 spike
505 protein modulate the virus affinity to the human ACE2 receptor, an in silico analysis. *EXCLI
506 journal* **2021**, *20*, 585-600, doi:10.17179/excli2021-3471.

507 55. Weisblum, Y.; Schmidt, F.; Zhang, F.; DaSilva, J.; Poston, D.; Lorenzi, J.C.C.; Muecksch, F.;
508 Rutkowska, M.; Hoffmann, H.-H.; Michailidis, E.; et al. Escape from neutralizing antibodies by
509 SARS-CoV-2 spike protein variants. *eLife* **2020**, *28*, e61312, doi:10.7554/eLife.61312.

510 56. Saifi, S.; Ravi, V.; Sharma, S.; Swaminathan, A.; Chauhan, N.S.; Pandey, R. SARS-CoV-2 VOCs,
511 Mutational diversity and clinical outcome: Are they modulating drug efficacy by altered
512 binding strength? *Genomics* **2022**, *114*, 110466, doi:10.1016/j.ygeno.2022.110466.

513 57. Focosi, D.; Maggi, F. Recombination in Coronaviruses, with a focus on SARS-CoV-2. *Viruses*
514 **2022**, *14*, 1239.

515 58. Roemer, C.H., R; Frohberg, N.; Sakaguchi, H.; Gueli, F.; Peacock, T. SARS-CoV-2 evolution,
516 post-Omicron. Available online: <https://virological.org/t/sars-cov-2-evolution-post-omicron/911> (accessed on November 26).

517 59. Lambisia, A.; Nyiro, J.; Morobe, J.; Makori, T.; Ndwiga, L.; Mburu, M.; Moraa, E.; Musyoki, J.;
518 Murunga, N.; Bejon, P.; et al. Detection of a SARS-CoV-2 Beta-like Variant with Additional
519 Mutations in Coastal Kenya after >1 Year of Disappearance. Available online:
520 <https://virological.org/t/detection-of-a-sars-cov-2-beta-like-variant-with-additional-mutations-in-coastal-kenya-after-1-year-of-disappearance/910> (accessed on November 26).

521 60. Sullivan, D.J.; Franchini, M.; Joyner, M.J.; Casadevall, A.; Focosi, D. Analysis of anti-Omicron
522 neutralizing antibody titers in different convalescent plasma sources. *Nat Comm* **2022**, *13*,
523 6478, doi:10.1038/s41467-022-33864-y.

524 61. Sullivan, D.J.; Franchini, M.; Senefeld, J.W.; Joyner, M.J.; Casadevall, A.; Focosi, D. Plasma
525 after both SARS-CoV-2 boosted vaccination and COVID-19 potently neutralizes BQ1.1 and
526 XBB. **2022**, *2022.2011.2025.517977*, doi:10.1101/2022.11.25.517977 %J bioRxiv.

527 62. FDA Announces Bebtelovimab is Not Currently Authorized in Any US Region. Accessed online
528 at <https://www.fda.gov/drugs/drug-safety-and-availability/fda-announces-bebtelovimab-not-currently-authorized-any-us-region> on December 1, 2022.

529 63. FDA Statement. January 24, 2022. Coronavirus (COVID-19) Update: FDA Limits Use of Certain
530 Monoclonal Antibodies to Treat COVID-19 Due to the Omicron Variant. Accessed online at
531 <https://www.fda.gov/news-events/press-announcements/coronavirus-covid-19-update-fda-limits-use-certain-monoclonal-antibodies-treat-covid-19-due-omicron> on February 3, .

532 64. FDA updates Sotrovimab emergency use authorization. March 30, 2022. Accessed online at
533 <https://www.fda.gov/drugs/drug-safety-and-availability/fda-updates-sotrovimab-emergency-use-authorization> on April 26, 2022.

534 65. FDA releases important information about risk of COVID-19 due to certain variants not
535 neutralized by Evusheld. Accessed online at <https://www.fda.gov/drugs/drug-safety-and-availability/fda-releases-important-information-about-risk-covid-19-due-certain-variants-not-neutralized-evusheld#:~:text=Therefore%2C%20on%20June%202029%2C%202022,if%20patients%20need%20ongoing%20protection.> on October 10, 2022.

536 66. Senefeld, J.W.; Klassen, S.A.; Ford, S.K.; Senese, K.A.; Wiggins, C.C.; Bostrom, B.C.;
537 Thompson, M.A.; Baker, S.E.; Nicholson, W.T.; Johnson, P.W.; et al. Use of convalescent
538 plasma in COVID-19 patients with immunosuppression. *Transfusion* **2021**, *61*, 2503-2511,
539 doi:10.1111/trf.16525.

540 67. Chen, C.; Nadeau, S.; Yared, M.; Voinov, P.; Xie, N.; Roemer, C.; Stadler, T. CoV-Spectrum:
541 analysis of globally shared SARS-CoV-2 data to identify and characterize new variants.
542 *Bioinformatics* **2021**, *38*, 1735-1737, doi:10.1093/bioinformatics/btab856 %J Bioinformatics.

543

544

545

546

547

548

549

550

551

552

553 68. Hadfield, J.; Megill, C.; Bell, S.M.; Huddleston, J.; Potter, B.; Callender, C.; Sagulenko, P.;
554 Bedford, T.; Neher, R.A. Nextstrain: real-time tracking of pathogen evolution. *Bioinformatics*
555 **2018**, *34*, 4121-4123, doi:10.1093/bioinformatics/bty407 %J Bioinformatics.

556

557

Table 1

558

559

560

561

562

Heatmap of selected Spike RBD mutations in Omicron sublineages and their impact on authorized therapeutic anti-Spike mAbs. BAM: bamlanivimab; ETE: etesevimab; CAS: casirivimab; IMD: imdevimab; TIX: tixagevimab; CIL: cilgavimab; SOT: sotrovimab; BEB: bebtelovimab; REG: regdanvimab. Data sourced from the Stanford University Coronavirus and Antiviral Resistance Database (accessed online at <https://covdb.stanford.edu/search-drdb> on November 30, 2022). Green means fold-reductions < 5; Orange means fold-reduction 5-100 ; Red means fold-reduction in IC₅₀ > 100 compared to wild-type; blank means no data available.

Spike mutation		Main lineages		BAM	ETE	CAS	IMD	CIL	TIX	SOT	BEB	REG
R346X	T	BS.1.*, BP.1, DD.1, BJ.1, BL.1.*, BL.2.*, BL.5, BA.2.75.2.* (CA.*), BM.1.1.* (CJ.* and CV.*), BM.4.1.1.1.* (CH.*), BR.2.* and BR.3, BN.1, BA.2.75.6.* (BY.*), BA.2.75.9.* (CY.*), BA.2.76, BA.4.1.8 and BA.4.1.9, CS.1, BA.4.6.* (DC.*), BA.4.7, BA.5.1.18 and BA.5.1.20, DE.2, BA.5.1.26.* (CU.*), BA.5.1.27 and BA.5.1.28, BF.7.*, BF.11.*, BA.5.2.6.* (CP.*), BA.5.2.13.* (CR.*), BA.5.2.25.* (DA.*), BA.5.2.39, BQ.1.1.* (CZ.*, CW.*, DK.*), BE.1.2.*, BE.1.4.2, BE.4.1.* (CQ.*), BE.5, BE.6 and BE.7, XBB.*, XBD, XBE, XBF, XBG										
	E	BA.5.6.4										
	I	BF.33, CE.1										
	R	BA.5.2.25, DB.2										
	S	BL.5, BF.13, BQ.1.21, BE.6										
K444X	M	CA.3.1, BR.1.*, BA.5.2.7, CY.1, BU.1, CG.1, BQ.1.17										
	N	BA.2.38.*, BA.4.6.3, BA.5.1.29, BV.2, BA.5.2.24, CK.* (DG.*), BE.4.2										
	R	BA.2.3.20.* (CM.*), CS.1, BF.16, BA.5.2.18, CR.1.*, CR.2, BA.5.2.41, CQ.1.*, XBB.4.*										
	T	CH.1.*, BR.4, BA.5.2.25, DB.1, DB.2, BA.5.2.36.* (CT.1), BE.1.1.1, BQ.1.* (CZ.*, CW.*, DK.*), BQ.2, BE.9,										

		BA.5.6.2.* (BW.1)									
V445	A	BA.4.6.2, BF.25, CP.1.1, BU.2, CR.1.2, , BA.5.2.23, BE.1.2.1, BE.1.4.3, CQ.2			Yellow	Red	Yellow		Green	Red	
	P	BJ.1, XBB.*									
G446	D	BA.5.2.30, CD.1								69	
	G	BR.4									
	S	BA.1.*, CM.8.*, BJ.1, BA.2.10.4, BH.1, BA.2.75.* (BL.* , CA.* , BM.* , CJ.* , CV.* , CH.* , BR.* , BN.* , BY.* , CB.*), BF.3.1, CP.1.3, CQ.1, XBB.* , XBC, XBD, XBF			Green	Red	Yellow	Green			
N450D		BU.3, CN.1, BA.5.2.32, BA.5.2.40, CC.1			Green	Red	Red				
L452X	L	XBD									
	M	BP.1, BA.2.3.20.* (CM.*), XBC.1									
	Q	BH.1, BA.2.75.8									
	R	BS.1.* , CA.1, CA.3.1, CA.7, CV.1, CH.1.1, BA.2.75.4.* (BR.*), BY.1.1.* , BA.4.* (CS.* , DC.*), BA.5.* (BT.* , DH.* , DE.* , CU.* , CL.* , BF.* , BZ.* , CP.* , CY.* , BU.* , CR.* , BV.* , CN.* , CK.* , DG.* , DB.* , CG.* , CF.* , CD.* , CE.* , CT.* , DA.* , BE.* , BQ.* , CZ.* , CW.* , CC.* , CQ.* , BW.* , DK.*), XBE, XBG	Red	Green	Green	Green	Green	Green	Red		
N460X	K	BS.1.* , BA.2.3.20.* (CM.*), DD.1, BA.2.75.* (BL.* , CA.* , BM.* , CJ.* , CV.* , CH.* , BR.* , BN.* , BY.* , CB.*), BA.4.6.3, CL.1, BF.33, CY.1, BU.1, CK.1, CK.2.* , DG.1, CK.3, DB.1, BQ.1.* (CZ.* , CW.* , DK.*), BE.4.2, BE.9, BW.1, XBB.* , XBD, XBF	Green	Red	Green	Green	Green	Green	Green		
	S	DC.1	Green	Red	Green	Green	Green	Green	Green	Green	
	Y	CP.3	Green	Red	Green	Green	Green	Green	Green	Green	
F486X	I	BM.2.3, BR.2.* , BF.7.12, BF.12							Green		

	P	BA.2.10.4, CA.4, CJ.1, XBB.1.5, XBC.*, XBF									
	S	BA.2.75.2.* (CA.*), BM.1.* (CV.*), BM.4.1.* (CH.*), BR.1.2, BY.1.*, BA.2.75.7, XBB.*, XBD			Red	Green		Red			
	V	BM.2.1, CB.1, BA.4.* (CS.*, DC.*), BA.5.* (BT.* , DH.* , DE.* , CU.* , CL.* , BF.* , BZ.* , CP.* , CY.* , BU.* , CR.* , BV.* , CN.* , CK.* , DG.* , DB.* , CG.* , CF.* , CD.* , CE.* , CT.* , DA.* , BE.* , BQ.* , CZ.* , CW.* , CC.* , CQ.* , BW.* , DK.*), XBE, XBG	Red	Yellow	Red	Green		Red	Green	Green	
F490X	I	CZ.1									
	L	BL.1.3	Red	Green	Green				Green	Green	
	S	BM.1.1.1.* (CJ.1), BN.1.* , BN.2.1., BN.3.1, BN.4, XBB.* , XBF	Red	Green	Green				Green	Green	
	V	BJ.1, BL.1.4									
R493X	L	BA.2.3.21.1	Yellow	Green					Green		
	Q	BA.2.10.4, BA.2.75.* (BL.* , CA.* , BM.* , CJ.* , CV.* , CH.* , BR.* , BN.* , BY.* , CB.*), BA.4.* (CS.* , DC.*), BA.5.* (BT.* , DH.* , DE.* , CU.* , CL.* , BF.* , BZ.* , CP.* , CY.* , BU.* , CR.* , BV.* , CN.* , CK.* , DG.* , DB.* , CG.* , CF.* , CD.* , CE.* , CT.* , DA.* , BE.* , BQ.* , CZ.* , CW.* , CC.* , CQ.* , BW.* , DK.*), XBB.* , XBC.* , XBD, XBE, XBF, XBG									
S494P		BA.2.10.4, CA.2, BN.1.* , BY.1.2.1, BQ.1.1.11, BQ.1.1.12, BQ.1.19	Red	Green	Green		Green		Green	Green	

564

Supplementary Table 1

565

566

Occurrence of selected amino acid mutations associated with immune escape within the Spike protein of SARS-CoV-2 in BA.2 and BA.4/5 Omicron sublineages. Modified from https://docs.google.com/spreadsheets/d/1OTWogpyvWNTIK0ww7TlDcl4l_SkZt3Z8nYiSp2YARys/edit?usp=sharing

PANGO lineage	nickname	Y 144del	R 346	K 356	K 444	V 445	G 446	N 450	L 452	N 460	F 486	F 490	R 493	S 494
BA.1							S							
BA.1.1				K			S							
BA.2														
BA.2.3														
BA.2.3.2														
BS.1				T					R				Q	
BS.1.1				T	T				R				Q	
BS.1.2				T					R				Q	
BA.2.3.16														
BP.1				T					M				Q	
BA.2.3.20	Basilisk					R		D	M				Q	
CM.1						R		D	M				Q	
CM.2						R		D	M				Q	
CM.3						R		D	M				Q	
CM.4						R		D	M				Q	
CM.5						R		D	M				Q	
CM.5.1						R		D	M				Q	
CM.6						R		D	M				Q	
CM.6.1						R		D	M				Q	
CM.7						R		D	M			S		
CM.8						R		S	D	M			Q	
CM.8.1						R		S	D	M	K	S		

CM.9					R	D	M	K					
BA.2.3.21				T									
DD.1									K				
BA.2.10													
BA.2.10.1													
BJ.1	Argus		T		P					V			P
BA.2.10.4											P		
BA.2.38					N								
BA.2.38.1					N								
BA.2.38.2					N								
BA.2.38.3								Q					
BH.1									K				
BA.2.38.4									K				
BA.2.75	Centaurus			T					K				
BA.2.75.1				T					K				
BL.1				T					K				
BL.1.1				T					K				
BL.1.2				T					K				
BL.1.3				T					K				
BL.1.4				T					K				
BL.2				T					K				
BL.2.1				T					K				
BL.3									K				
BL.4									K				
BL.5			S						K		S		
BA.2.75.2	Chiron		T					R	K	S			P
CA.1			T										
CA.2			T										

CA.3		T			S			K	S		Q
CA.3.1		T		M	S		R	K	S		Q
CA.4		T			S			K	P		Q
CA.5		T			S			K	S		Q
CA.6		T			S			K	S		Q
CA.7		T			S		R	K	S		Q
BA.2.75.3					S			K			Q
BM.1					S			K	S		Q
BM.1.1		T			S			K	S		Q
BM.1.1.1	Mimas	T			S			K	S	S	Q
CJ.1		T			S			K	P	S	Q
BM.1.1.2		T			S			K	S		Q
BM.1.1.3		T			S			K	S		Q
CV.1		T			S		R	K	S		Q
BM.2		T			S			K			Q
BM.2.1		T			S			K		V	Q
BM.2.2		T			S			K			Q
BM.2.3		T			S			K	I		Q
BM.3					S			K			Q
BM.4					S			K			Q
BM.4.1					S			K	S		Q
BM.4.1.1		T			S			K	S		Q
CH.1		T		T	S			K	S		Q
CH.1.1		T		T	S		R	K	S		Q
CH.2		T			S			K	S		Q
BM.5					S			K			Q
BM.6					S			K			Q
BA.2.75.4					S		R	K			Q

BR.1					M		S	R	K			Q
BR.1.1					M		S	R	K			Q
BR.1.2					M		S	R	K	S		Q
BR.2			T				S	R	K	I		Q
BR.2.1			T				S	R	K	I		Q
BR.3			T				S	R	K			Q
BR.4				T			G	R	K			Q
BA.2.75.5				T			S		K			Q
BN.1	Hydra		T	T			S		K	S	Q	
BN.1.1			T	T			S		K	S	Q	P
BN.1.1.1			T	T			S		K	S	Q	P
BN.1.2			T	T			S		K	S	Q	
BN.1.2.1			T	T			S		K	S	Q	
BN.1.3			T	T			S		K	S	Q	
BN.1.3.1			T	T			S		K	S	Q	
BN.1.4			T	T			S		K	S	Q	
BN.1.5			T	T			S		K	S	Q	
BN.1.6			T	T			S		K	S	Q	
BN.1.7			T	T			S		K	S	Q	
BN.2				T			S		K			Q
BN.2.1				T			S		K	S	Q	
BN.3				T			S	D	K			Q
BN.3.1				T			S	D	K	S	Q	
BN.4				T			S		K	S	Q	
BN.5				T			S		K			Q
BN.6				T			S		K			Q
BA.2.75.6	Dictys		T				S		K			Q
BY.1			T				S		K	S		Q

BY.1.1		T			S	R	K	S	Q
BY.1.1.1		T			S	R	K	S	Q
BY.1.2		T			S		K	S	Q
BY.1.2.1		T			S		K	S	Q
BA.2.75.7					S		K	S	Q
BA.2.75.8					S	Q	K		Q
BA.2.75.9		T			S		K		Q
CB.1		T			S		K	V	Q
BA.2.75.10					S		K		Q
BA.2.76		T							
BA.4						R		V	Q
BA.4.1						R		V	Q
BA.4.1.8		T				R		V	Q
BA.4.1.9	Cetus	T				R		V	Q
BA.4.1.10		T				R		V	Q
CS.1		T	R			R		V	Q
BA.4.6	Aeterna	T				R		V	Q
BA.4.6.1		T				R		V	Q
BA.4.6.2		T	A			R		V	Q
BA.4.6.3		T	N			R	K	V	Q
BA.4.6.4		T				R		V	Q
BA.4.6.5		T				R		V	Q
DC.1		T				R	S	V	Q
BA.4.7		T				R		V	Q
BA.4.8						R		V	Q
BA.5						R		V	Q
BA.5.1	Sphinx					R		V	Q
BA.5.1.18		T				R		V	Q

BA.5.1.19					R		V		Q
BA.5.1.20		T			R		V		Q
BA.5.1.21					R		V		Q
BT.1					R		V		Q
BT.2					R		V		Q
BA.5.1.22					R		V		Q
DH.1					R		V		Q
BA.5.1.23					R		V		Q
DE.1					R		V		Q
DE.2		T			R		V		Q
BA.5.1.24					R		V		Q
BA.5.1.25					R		V		Q
BA.5.1.26		T			R		V		Q
CU.1		T			R		V		Q
BA.5.1.27		T			R		V		Q
BA.5.1.28		T			R		V		Q
BA.5.1.29			N		R		V		Q
CL.1					R	K	V		Q
BA.5.1.30					R		V		Q
BA.5.2	Triton				R		V		Q
BA.5.2.1					R		V		Q
BF.1					R		V		Q
BF.1.1					R		V		Q
BF.2					R		V		Q
BF.3				S	R		V		Q
BF.3.1					R		V		Q
BF.4					R		V		Q
BF.5					R		V		Q

BF.6						R	V	Q
BF.7	Minotaur	T				R	V	Q
BF.7.1		T				R	V	Q
BF.7.2		T				R	I	Q
BF.7.3		T				R	V	Q
BF.7.4		T				R	V	Q
BF.7.4.1		T				R	V	Q
BF.7.4.2		T				R	V	Q
BF.7.5		T				R	V	Q
BF.7.5.1		T				R	V	Q
BF.7.6		T				R	V	Q
BF.7.7		T				R	V	Q
BF.7.8		T				R	V	Q
BF.7.9		T				R	V	Q
BF.7.10		T				R	V	Q
BF.7.11		T				R	V	Q
BF.7.12		T				R	V	Q
BF.7.13		T				R	V	Q
BF.7.13.1		T				R	V	Q
BF.7.13.2		T				R	V	Q
BF.8						R	V	Q
BF.9						R	V	Q
BF.10						R	V	Q
BF.11	Python	T				R	V	Q
BF.11.1		T				R	V	Q
BF.11.2		T				R	V	Q
BF.11.3		T				R	V	Q
BF.11.4		T				R	V	Q

BF.11.5		T			R		V		Q
BF.12					R		I		Q
BF.13		S			R		V		Q
BF.14					D	R	V		Q
BF.15						R	V		Q
BF.16			R			R	V		Q
BF.17						R	V		Q
BF.18						R	V		Q
BF.19						R	V		Q
BF.20						R	V		Q
BF.21						R	V		Q
BF.22						R	V		Q
BF.23						R	V		Q
BF.24						R	V		Q
BF.25			A			R	V		Q
BF.26						R	V		Q
BF.27						R	V		Q
BF.28						R	V		Q
BF.29						R	V		Q
BF.30		T				R	V		Q
BF.31						R	V		Q
BF.31.1						R	V		Q
BF.32					D	R	V		Q
BF.33		I				R	V		Q
BF.34		T				R	V		Q
BA.5.2.3						R	V		Q
BZ.1						R	V		Q
BA.5.2.6		T				R	V		Q

CP.1		T				R		V		Q
CP.1.1		T				R		V		Q
CP.1.2		T				R		V		Q
CP.1.3		T				S		V		Q
CP.2		T					R	V		Q
CP.3		T					R	V		Q
CP.4		T					R	V		Q
CP.5		T					R	V		Q
CP.6		T					R	V		Q
BA.5.2.7				M			R	V		Q
CY.1				M			R	K	V	Q
BA.5.2.13		T					R	V		Q
BA.5.2.16							R	V		Q
BU.1				M			R	K	V	Q
BU.2					A		R	V		Q
BU.3						D	R	V		Q
BA.5.2.18				R			R	V		Q
CR.1		T		R			R	V		Q
CR.1.1		T		R			R	V		Q
CR.1.2		T		R	A		R	V		Q
CR.2				R			R	V		Q
BA.5.2.19							R	V		Q
BA.5.2.20							R	V		Q
BV.1							R	V		Q
BV.2				N			R	V		Q
BA.5.2.21							R	V		Q
CN.1						D	R	V		Q
BA.5.2.22							R	V		Q

BA.5.2.23					A		R		V		Q
BA.5.2.24					N		R		V		Q
CK.1					N		R		V		Q
CK.2					N		R		V		Q
CK.2.1					N		R		V		Q
CK.2.1.1					N		R		V		Q
DG.1					N		R		V		Q
CK.3					N		R		V		Q
BA.5.2.25		R		T			R		V		Q
DB.1		T		T			R		V		Q
DB.2		R		T			R		V		Q
BA.5.2.26					M		R		V		Q
CG.1							R		V		Q
BA.5.2.27							R		V		Q
CF.1							R		V		Q
BA.5.2.28							R		V		Q
BA.5.2.29							R		V		Q
BA.5.2.30						D	R		V		Q
BA.5.2.31							R		V		Q
CD.1						D	R		V		Q
CD.2							R		V		Q
BA.5.2.32							D	R	V		Q
BA.5.2.33		I					R		V		Q
CE.1							R		V		Q
BA.5.2.34		T					R		V		Q
BA.5.2.35		T					R		V		Q
BA.5.2.36				T			R		V		Q
CT.1			T	T			R		V		Q

BA.5.2.37						R		V		Q
BA.5.2.38						R		V		Q
DA.1		T				R		V		Q
BA.5.2.39		T				R		V		Q
BA.5.2.40			R		D	R		V		Q
BA.5.2.41						R		V		Q
BA.5.3						R		V		Q
BA.5.3.1						R		V		Q
BE.1						R		V		Q
BE.1.1			T			R		V		Q
BE.1.1.1			T			R		V		Q
BQ.1	Typhon		T			R	K	V		Q
BQ.1.1	Cerberus	T	T			R	K	V		Q
BQ.1.1.1		T	T			R	K	V		Q
CZ.1		T	T			R	K	V	I	Q
BQ.1.1.2		T	T			R	K	V		Q
BQ.1.1.3		T	T			R	K	V		Q
BQ.1.1.4		T	T			R	K	V		Q
BQ.1.1.5		T	T			R	K	V		Q
BQ.1.1.6		T	T			R	K	V		Q
BQ.1.1.7		T	T			R	K	V		Q
BQ.1.1.8		T	T			R	K	V		Q
BQ.1.1.9		T	T			R	K	V		Q
BQ.1.1.10		T	T			R	K	V		Q
BQ.1.1.11		T	T			R	K	V		Q
BQ.1.1.12		T	T			R	K	V		Q
BQ.1.1.13		T	T			R	K	V		Q
BQ.1.1.14		T	T			R	K	V		Q

CW.1			T		T		S	R	K	V		Q
BQ.1.1.15			T		T			R	K	V		Q
BQ.1.1.16			T		T			R	K	V		Q
BQ.1.1.17			T		T			R	K	V		Q
BQ.1.1.18			T		T			R	K	V		Q
BQ.1.1.19			T		T			R	K	V		Q
BQ.1.1.20			T		T			R	K	V		Q
BQ.1.1.21			T		T			R	K	V		Q
BQ.1.1.22			T		T			R	K	V		Q
BQ.1.1.23			T		T			R	K	V		Q
BQ.1.1.24			T		T			R	K	V		Q
BQ.1.2					T			R	K	V		Q
BQ.1.3					T			R	K	V		Q
BQ.1.4					T			R	K	V		Q
BQ.1.5					T			R	K	V		Q
BQ.1.6					T			R	K	V		Q
BQ.1.7					T			R	K	V		Q
BQ.1.8					T			R	K	V		Q
BQ.1.8.1					T			R	K	V		Q
BQ.1.8.2					T			R	K	V		Q
BQ.1.9			T		T			R	K	V		Q
BQ.1.10					T			R	K	V		Q
BQ.1.10.1					T			R	K	V		Q
BQ.1.11					T			R	K	V		Q
BQ.1.12					T			R	K	V		Q
BQ.1.13					T			R	K	V		Q
BQ.1.14					T			R	K	V		Q
BQ.1.15					T			R	K	V		Q

BQ.1.16				T			R	K	V		Q
BQ.1.17				M			R	K	V		Q
BQ.1.18		T		T			R	K	V		Q
BQ.1.19				T			R	K	V		Q
BQ.1.20				T			R	K	V		Q
BQ.1.21		S		T			R	K	V		Q
BQ.1.22		T		T			R	K	V		Q
BQ.1.23				T			R	K	V		Q
BQ.1.24		T		T			R	K	V		Q
BQ.1.25		T		T			R	K	V		Q
BQ.1.26				T			R	K	V		Q
BQ.2				T			R		V		Q
BE.1.1.2							R		V		Q
CC.1						D	R		V		Q
BE.1.2		T					R		V		Q
BE.1.2.1		T			A		R		V		Q
BE.1.3							R		V		Q
BE.1.4							R		V		Q
BE.1.4.1							R		V		Q
BE.1.4.2		T					R		V		Q
BE.1.4.3					A		R		V		Q
BE.1.4.4							R		V		Q
BE.2							R		V		Q
BE.3							R		V		Q
BE.4							R		V		Q
BE.4.1		T					R		V		Q
BE.4.1.1		T		R			R		V		Q
CQ.1		T		R			R		V		Q

CQ.1.1		T		R		R		V		Q
CQ.2		T		R		R		V		Q
BE.4.2				N	A			K	V	Q
BE.5		T				R		V		Q
BE.6		S				R		V		Q
BE.7		T				R		V		Q
BE.8		T				R		V		Q
BE.9			T			R	K	V		Q
BA.5.3.5		T				R		V		Q
BA.5.5						R		V		Q
BA.5.5.3						R		V		Q
BA.5.6						R		V		Q
BA.5.6.2			T			R		V		Q
BW.1			T			R	K	V		Q
BA.5.6.3		T				R		V		Q
BA.5.6.4		E				R		V		Q
BA.5.10						R		V		Q
BA.5.10.1		T				R		V		Q
DF.1		T				R		V		Q
BA.5.11		T				R		V		Q
XBB	Gryphon	T		P	S		K	S	S	Q
XBB.1		T		P	S		K	S	S	Q
XBB.1.1		T		P	S		K	S	S	Q
XBB.1.2		T		P	S		K	S	S	Q
XBB.1.3		T		P	S		K	S	S	Q
XBB.1.4		T		P	S		K	S	S	Q
XBB.1.5		T		P	S		K	P	S	Q
XBB.2		T		P	S		K	S	S	Q

XBB.3		T		P	S			K	S	S	Q
XBB.3.1		T		P	S			K	S	S	Q
XBB.4		T		R	P	S		K	S	S	Q
XBB.4.1		T		R	P	S		K	S	S	Q
XBB.5		T		P	S			K	S	S	Q
XBC					S				P		Q
XBC.1					S		M		P		Q
XBC.2					S				P		Q
XBD		T			S		L	K	S		Q
XBE		T					R		V		Q
XBF		T			S			K	P		Q
XBG		T					R		V		Q

567

568

569

570

Figure 1

571 Radial tree of SARS-CoV-2 evolution, with branch length approximating divergence, showing that Omicron (light blue shadow) currently includes more than
572 45% of variations across 3045 genomes sampled between Dec 2019 and Nov 2022. Accessed online at <https://nextstrain.org/ncov/gisaid/global/all-time?l=radial&m=div> on November 26, 2022.

574

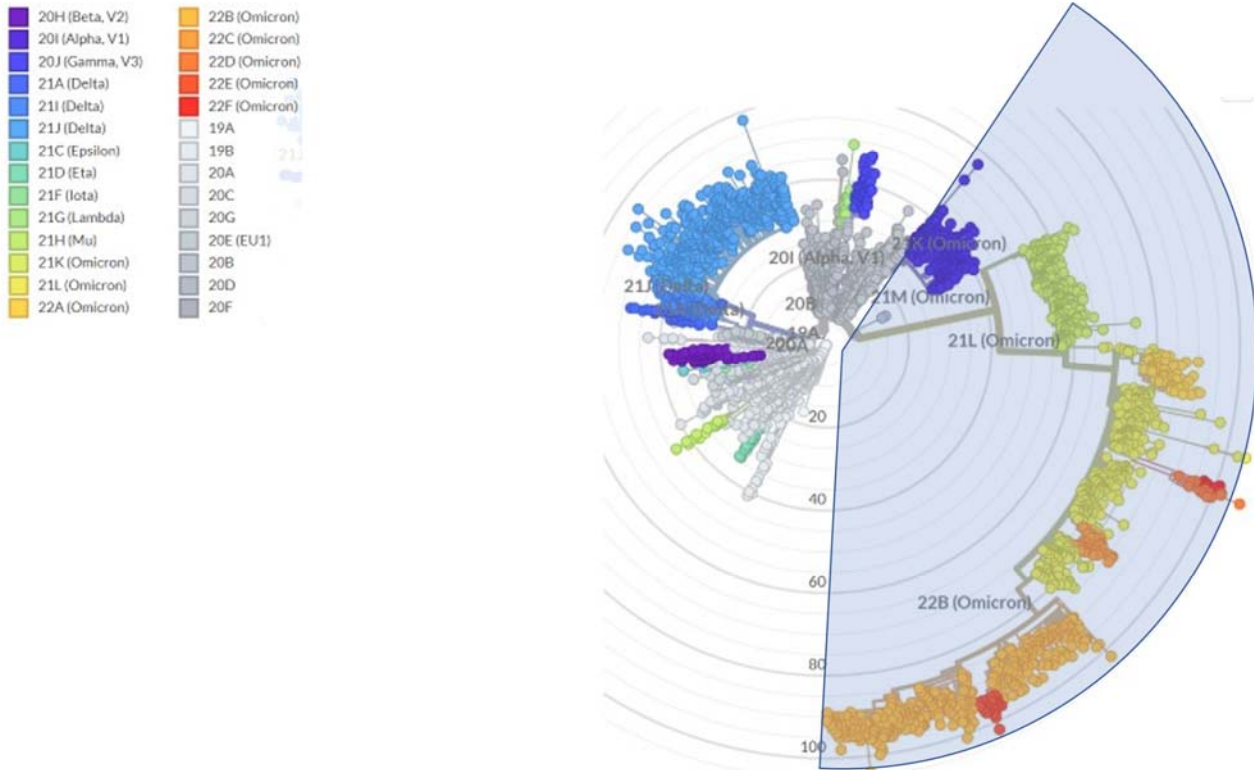
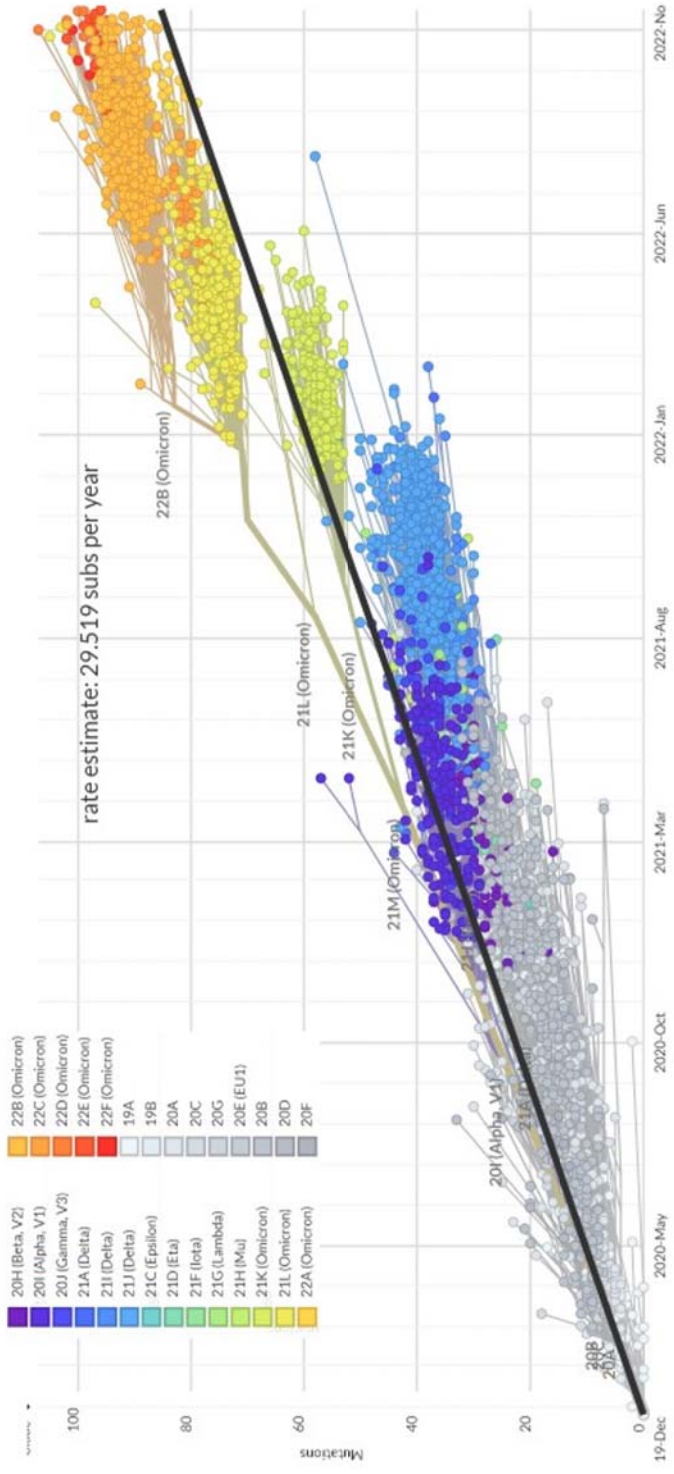


Figure 2 575

575 576 577

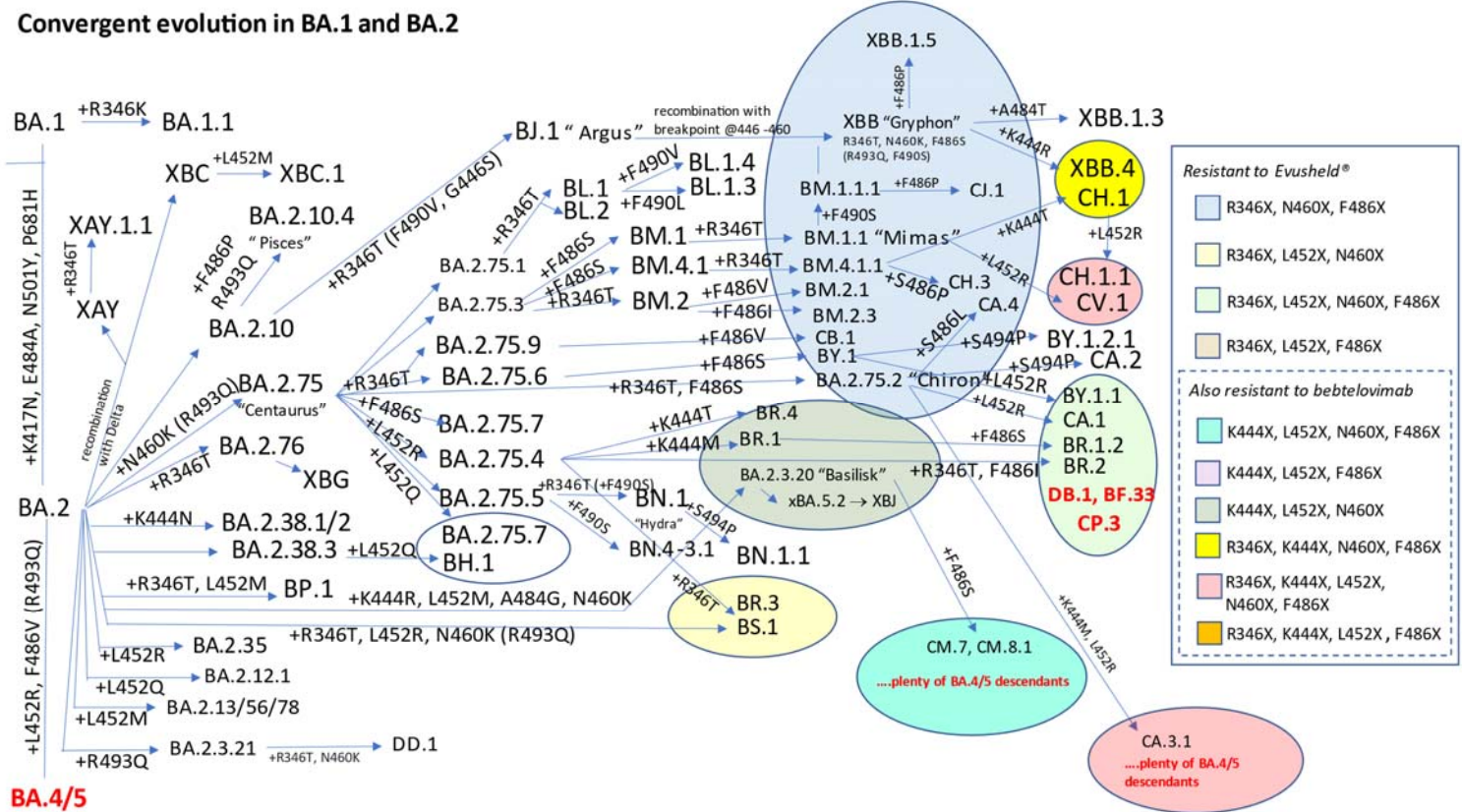
Clock tree of SARS-CoV-2 evolution, with regression line showing an increase in the estimate rate of substitutions per year across 3045 genomes sampled between Dec 2019 and Nov 2022. Accessed online at <https://nextstrain.org/hcov/gisaid/global/all-time?l=clock&m=div> on November 26, 2022.



579

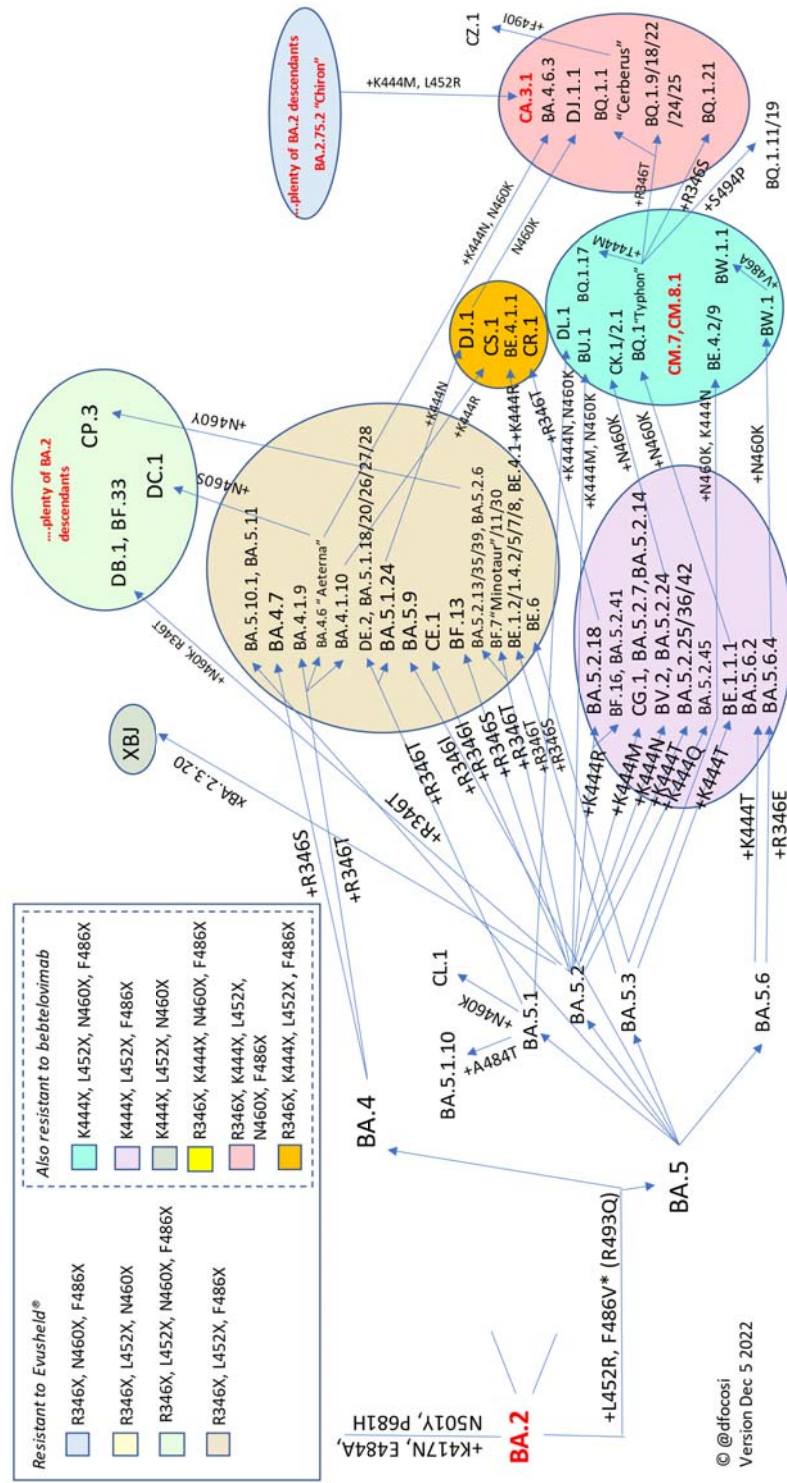
Figure 3

580 Diagram representing all SARS-CoV-2 Omicron sublineages designated by PANGOLIN as of November 26, 2022 for which at least one of the Spike RBD
 581 immune escaping mutations (R346X, K444X, L452X, N460X, F486X, or R493Q) represents a branching event. Mythological names introduced by Ryan T
 582 Gregory and used colloquially are also reported. Convergence towards combos of this mutations is noted, with different background colors representing
 583 different combinations. Resistance of each combination to clinically authorized anti-Spike mAbs is reported on the right box. For visualization purposes, the
 584 upper panel shows BA.1 and BA.2 evolution, while the lower panel shows BA.4/5 evolution.



585

Convergent evolution in BA.4/5



587

Figure 4

588

589

590

591

592

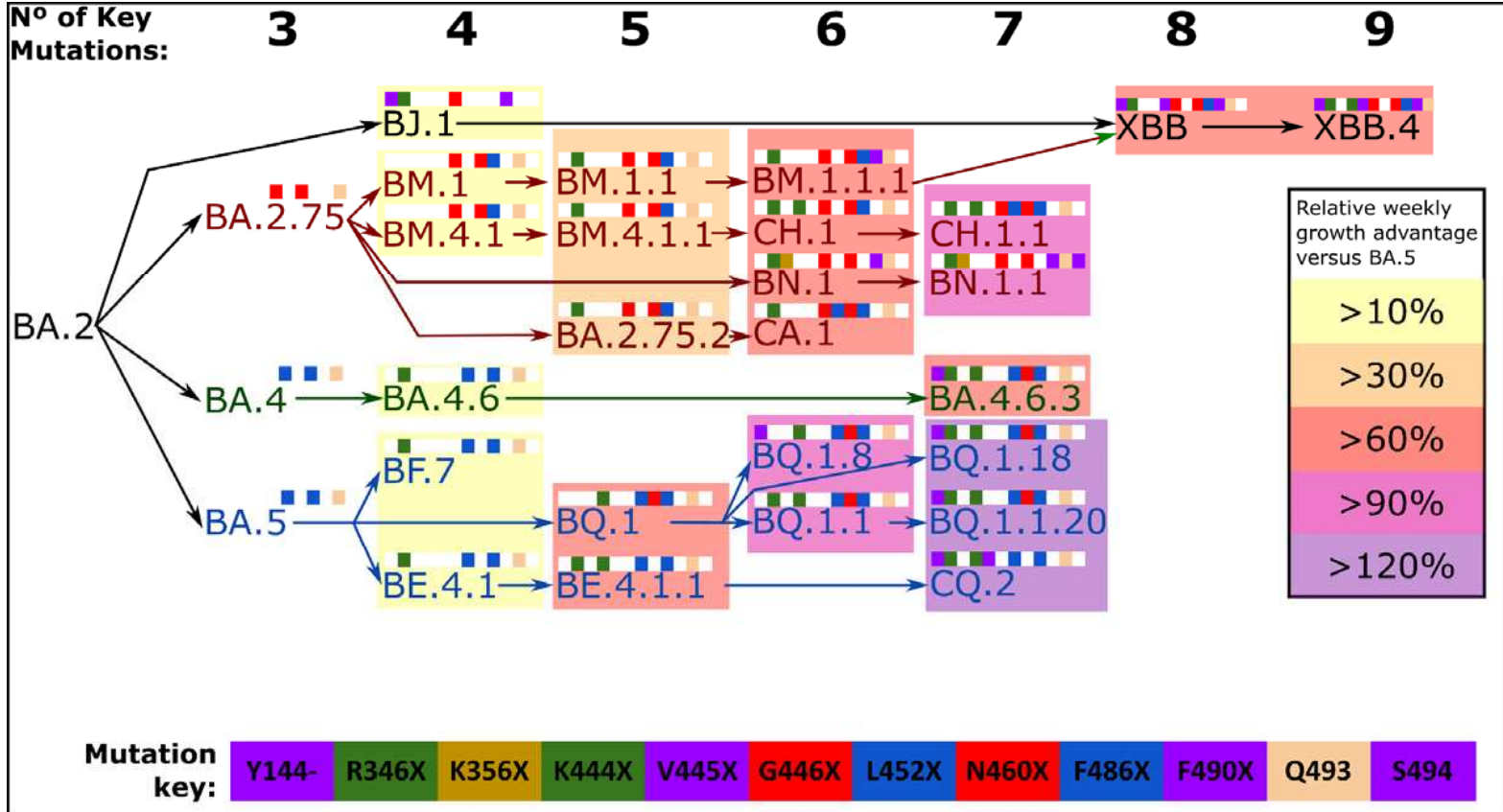
593 Step-wise accumulation of key Spike mutations involved in immune escape within SARS-CoV-2 Omicron sublineages increase the relative growth rate.

594 Lineage name text is color coded, where BA.5 descendants are in blue text, BA.4 descendants in green text and BA.2.75 descendants are in red text. Each

595 mutation is color coded as shown in the mutation key, and depicted as colored squares when present or white squares if absent. Number of key mutations

596 of each lineage is summarized at the top. Relative growth rates were calculated using BA.5 lineage as baseline, for groups of BA.4, BA.5, BA.2.75 and XBB

597 descendant lineages with each exact total number of key mutations. Relative growth rates were calculated using CoV-Spectrum [67]



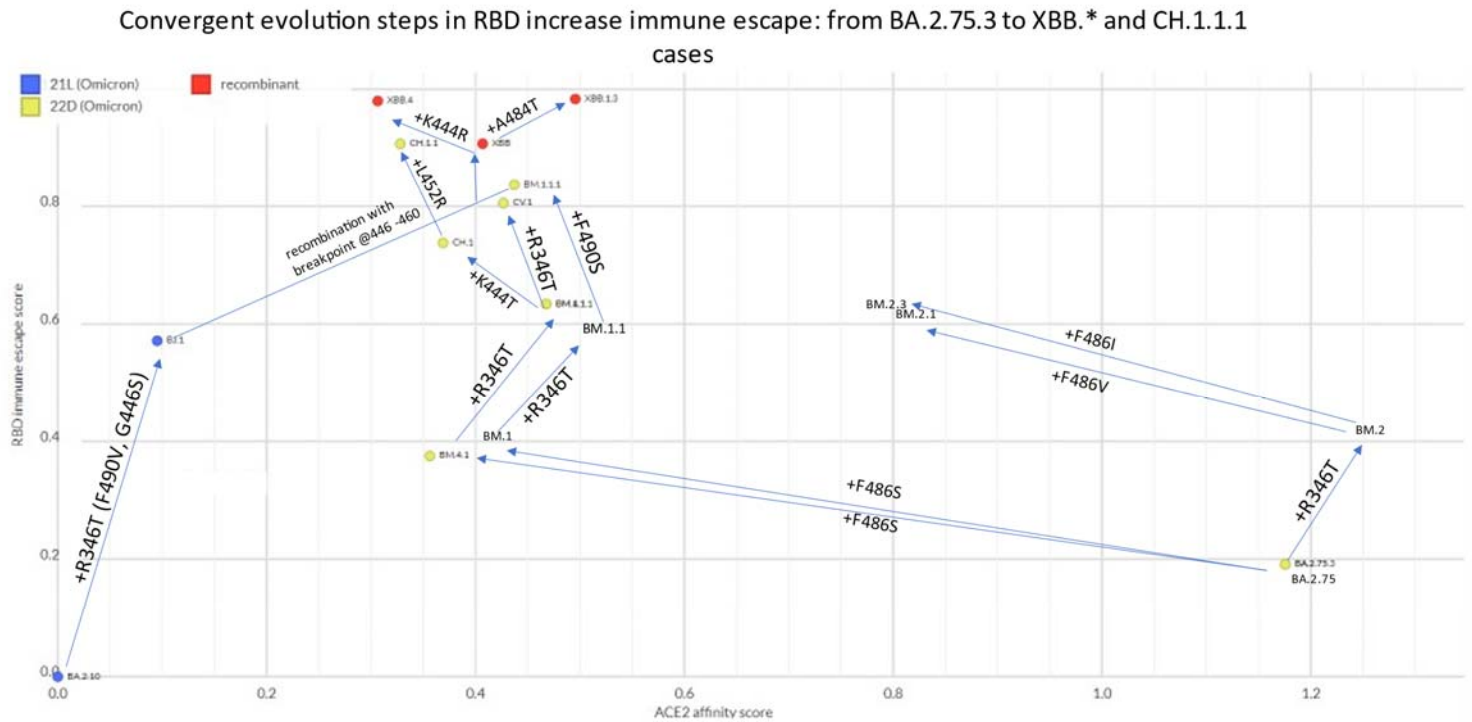
593

594

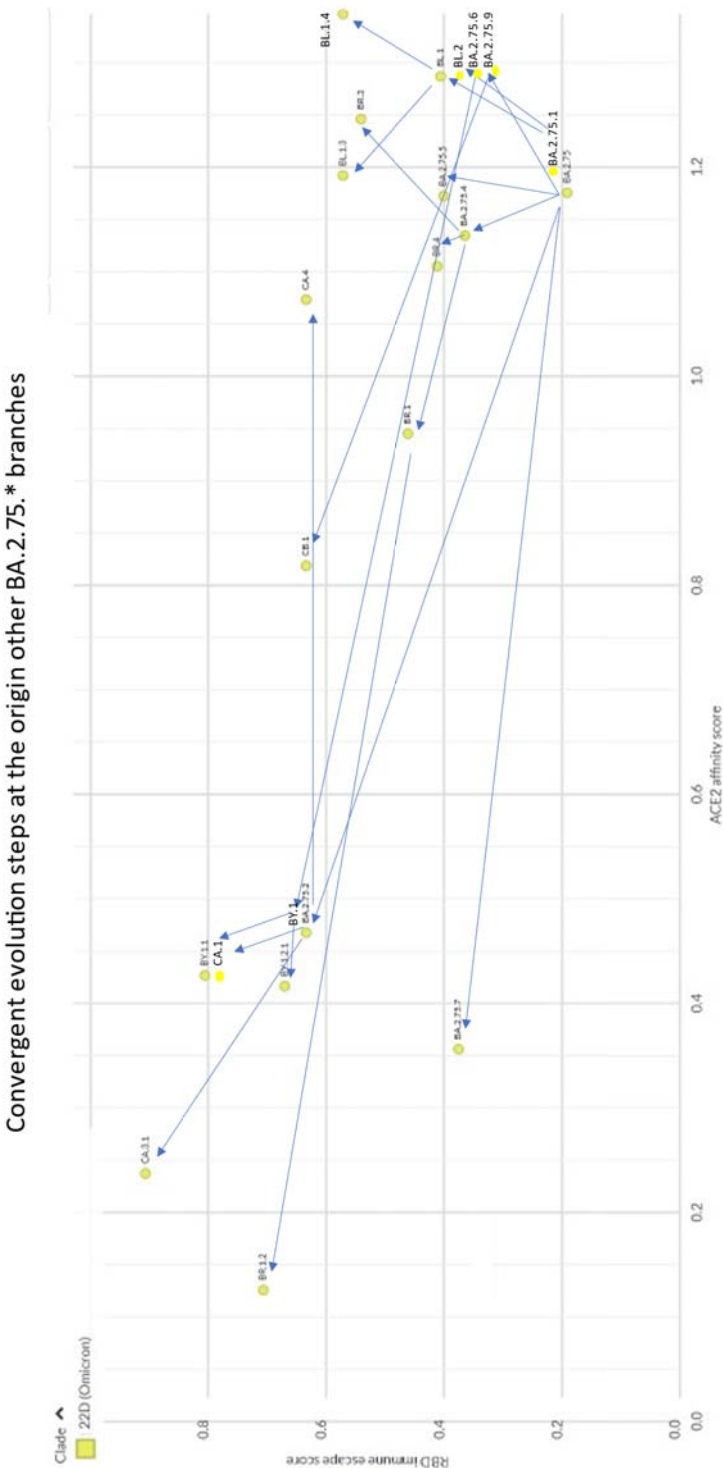
595

Figure 5

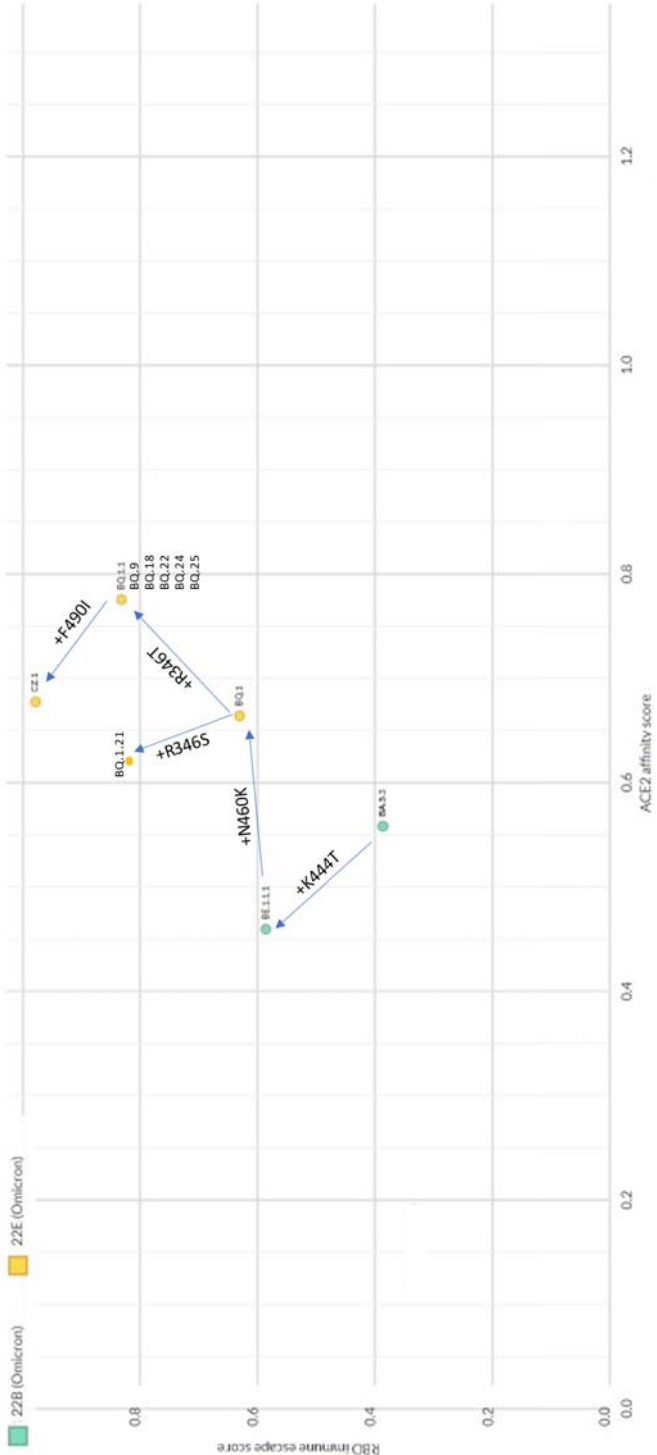
596 **Evolutionary steps at the basis of the major Omicron branches (CZ.1, XBB.* and CH.1.1.1, and other BA.2.75.* descendants), showing progressive increases**
 597 in RBD immune escape score (as calculated here: https://jbloomlab.github.io/SARS2_RBD_Ab_escape_maps/escape-calc/). Chart created on NextStrain [68]
 598 (https://next.nextstrain.org/staging/nextclade/sars-cov-2/21L?gmin=15&l=scatter&scatterX=ace2_binding&scatterY=immune_escape&showBranchLabels=all)



600



Convergent evolution steps in RBD increase immune escape: the CZ.1 case

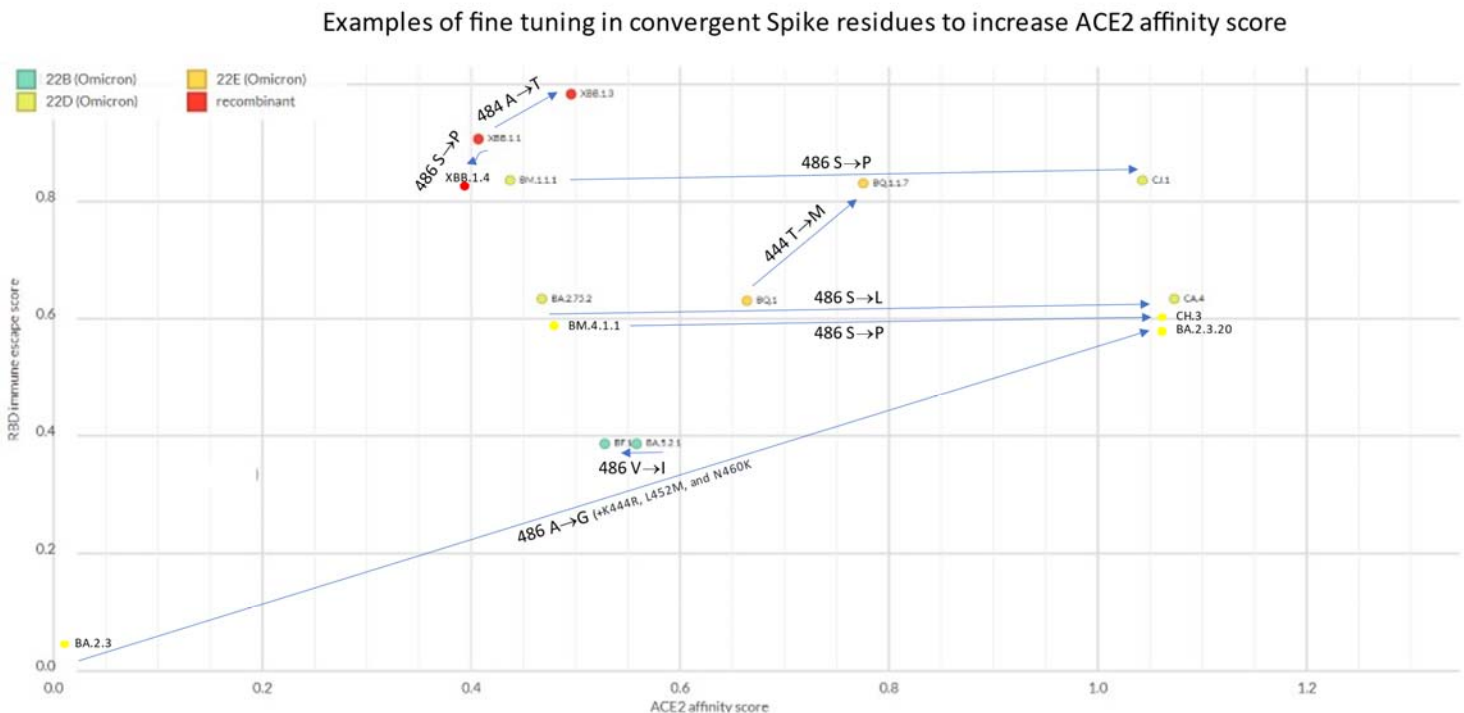


602

40

Figure 6

Sequential mutational events at the same Spike amino acid residues showing no change or progressive increases in ACE2 affinity score (as calculated here: https://github.com/jbloomlab/SARS-CoV-2-RBD_DMS_Omicron/blob/main/results/final_variant_scores/final_variant_scores.csv). Chart created on NextStrain [68] (https://next.nextstrain.org/staging/nextclade/sars-cov-2/21L?gmin=15&l=scatter&scatterX=ace2_binding&scatterY=immune_escape&showBranchLabels=all)



609

Figure 7

610

Mutually exclusive mutations at R346 and N450. The receptor binding domain of S is depicted in grey cartoon representation, with the receptor binding module (ACE2 interaction interface) highlighted in orange. Amino acids at the 346 and 450 positions are displayed as purple sticks. A zoomed-in view of the R346-N450 interaction in the ancestral domain, as well as the computationally modelled amino acid substitutions at those two positions, are portrayed in boxes to the right. In the wild-type sequence, the basic R346 sidechain interacts with the N450 residue through a pair of hydrogen bond interactions. N450D results in a similarly sized sidechain, but altered electrostatics. One hydrogen bond is maintained between the neutral oxygen of Asp and N_{ϵ} of Arg, and a new salt bridge is formed between the anionic deprotonated oxygen of Asp and the cationic center of the guanidino group of Arg. In the case of R346X, any substitution except lysine would result in a side chain that is significantly shorter and non-cationic, thus dissolving the interactions between N450 or other common substitutions at that position.

611

612

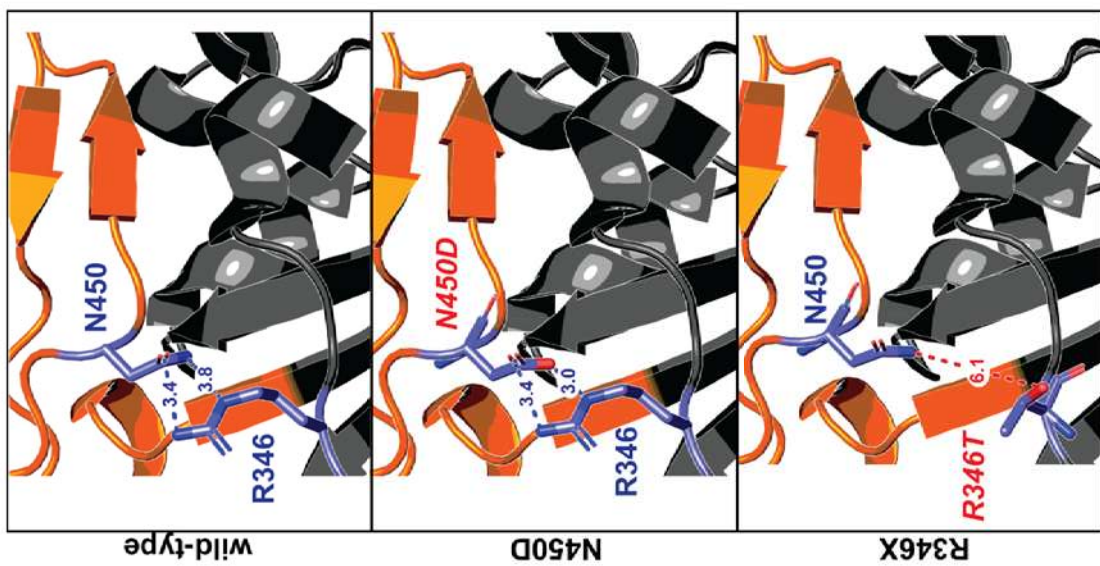
613

614

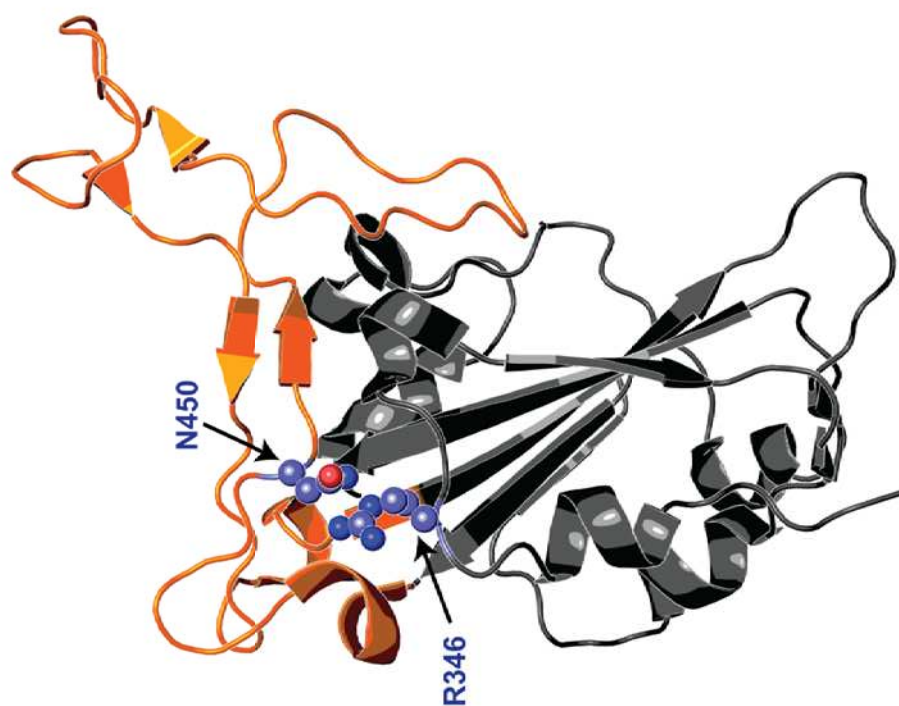
615

616

617



43



618

621
622 **Figure 8**
623 Prevalence of S:R346X mutations in the period 2020-08-27 – 2022-09-13 in UK versus France. Sourced from <https://cov-spectrum.org> on November 26, 2022. The blue area represents trends in Evusheld™ prescriptions in France and many other countries (but not UK).

